

Finding the FrameStack: Learning What to Remember for Non-Markovian Reinforcement Learning

Geraud Nangue Tasse¹, Matthew Riemer^{2,3}, Benjamin Rosman¹, Tim Klinger³

{geraud.nanguetassel, benjamin.rosman1}@wits.ac.za,
{mdriemer, tklinger}@us.ibm.com

¹**CSAM School, University of the Witwatersrand, ZA**

²**Mila, Université de Montréal, CA**

³**IBM Research, Yorktown Heights, NY**

Abstract

Recent success in developing increasingly general purpose agents based on sequence models has led to increased focus on the problem of deploying computationally limited agents within the vastly more complex real-world. A key challenge experienced in these more realistic domains is highly non-Markovian dependencies with respect to the agent’s observations, which are less common in small controlled domains. The predominant approach for dealing with this in the literature is to stack together a window of the most recent observations (*Frame Stacking*), but this window size must grow with the degree of non-Markovian dependencies, which results in prohibitive computational and memory requirements for both action inference and learning. In this paper, we are motivated by the insight that in many environments that are highly non-Markovian with respect to time, the environment only causally depends on a relatively small number of observations over that time-scale. A natural direction would then be to consider meta-algorithms that maintain relatively small adaptive stacks of memories such that it is possible to express highly non-Markovian dependencies with respect to time while considering fewer observations at each step and thus experience substantial savings in both compute and memory requirements. Hence, we propose a meta-algorithm (*Adaptive Stacking*) for achieving exactly that with convergence guarantees and quantify the reduced computation and memory constraints for MLP, LSTM, and Transformer-based agents. Our experiments utilize the classic T-Maze domain, which gives us direct control over the degree of non-Markovian dependencies in the environment. This allows us to demonstrate that an appropriate meta-algorithm can learn the removal of memories not predictive of future rewards and achieve convergence in the stack management policy without excessive removal of important experiences.

1 Introduction

Reinforcement learning (RL) agents are typically formulated under the Markov assumption: the agent’s current observation contains all information needed for optimal decision-making (Puterman, 2014). In practice, however, real-world environments are often partially observable—the agent’s immediate observation is an incomplete snapshot of the true state. This leads to non-Markovian dependencies over time, where past observations contain critical context for future decisions. Notably, Abel et al. (2021) proved that there exist certain tasks (for example expressed as desired behaviour specifications) that cannot be captured by any Markovian reward function. In other words, no memoryless reward can incentivise the correct behaviour for those tasks—agents must rely on histories of observations to infer hidden state information and resolve non-Markovian dependencies. This theoretical insight underlines that non-Markovian tasks are not just harder, but sometimes

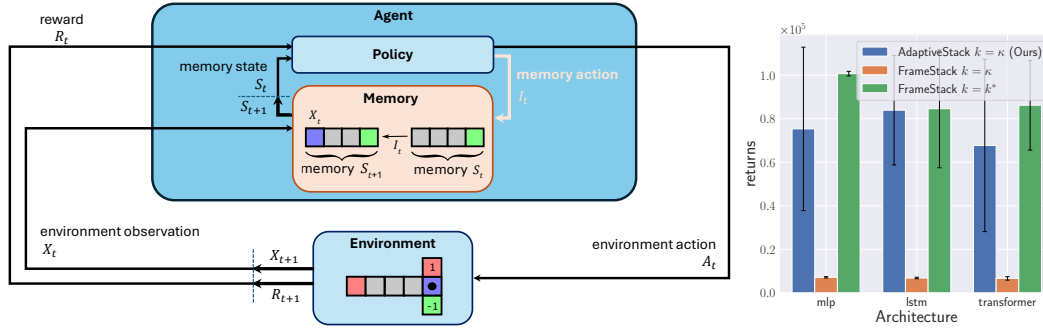


Figure 1: Learning what to remember using Adaptive Stacking. **(left)** Modification to the standard RL loop. **(right)** Performance of PPO on a Passive-TMaze with random lengths in [2, 16]. The stack size k needed for FrameStack is k^* , which scales with the maze length, whereas only $\kappa = 2$ are needed.

fundamentally require memory beyond the scope of standard Markov formulations. We are interested in such settings in big worlds (Javed & Sutton, 2024), where only a relatively small subset of past observations are relevant for optimal decision-making, but they are separated by large spans of time.

While RL has shown great success in a variety domains (Arulkumaran et al., 2017; Cao et al., 2024), handling such temporal dependencies remains a challenge especially for computationally limited agents operating in big worlds (Javed & Sutton, 2024). In practice, the most common approach to address this problem is *Frame Stacking* (FS), which is a FIFO short-term memory wherein a fixed context window of the most recent k^* observations (and actions) are concatenated. This is then used directly as policy input, or first used to infer hidden states typically using active inference (Friston, 2009; Sajid et al., 2021) or sequence models like recurrent neural networks (Hochreiter & Schmidhuber, 1997; Hausknecht & Stone, 2015), Transformers (Vaswani et al., 2017; Chen et al., 2021), and state space models (Gu et al., 2021; Samsami et al., 2024). Given knowledge of the nature of the temporal dependencies, for example when they are expressible as reward machines (Icarte et al., 2022; Bester et al., 2023), prior works also use such histories of observations and program synthesis to learn abstract state machines that compactly represent the memory and temporal dependencies (Toro Icarte et al., 2019; Hasanbeig et al., 2024). While such approaches based on FS are very effective in domains with short-term dependencies, such as in Atari games (Mnih et al., 2013) where 4 frames are enough to capture the motion of objects, they quickly become impractical in domains where relevant information may have occurred in an *unknown large* number of steps (Ni et al., 2023). Importantly, increasing k^* causes an exponential increase in the dimensionality of the observation space, leading to both a severe increase in compute and storage, and potentially poor sample efficiency and generalisation.¹

However, many tasks may not actually require remembering everything—often only a sparse subset of past observations is truly relevant for making optimal decisions. This insight aligns with findings in cognitive neuroscience: working memory in humans is known to have limited capacity and is thought to employ a selective gating mechanism that retains task-relevant information while filtering out irrelevant inputs (Unger et al., 2016). For example, a driver listening to a traffic report will update only the few road incidents relevant to her route into memory and ignore other trivial reports. Similarly, an RL agent with constrained memory should learn what to remember and what to forget. If the agent can identify which observations carry information critical for future reward, it could store just those and safely discard others, drastically reducing the burden on its memory and computation. Ideally, this is possible without sacrificing performance, but instead actually improving generalisation.

Driven by this insight, we make the following main contributions: 1. **Adaptive Stacking:** We propose *Adaptive Stacking* (AS), a general meta-algorithm that learns to selectively retain observations in a working memory of fixed size κ (Figure 1). When $\kappa \ll k^*$, this significantly improves compute and memory efficiency. It also leads to an exponential reduction in the size of the search space, which has implications for sample efficiency and generalisation. 2. **Theoretical analysis:** We then

¹See Appendix A for a detailed overview of related works.

prove that agents using this approach are guaranteed to converge to an optimal policy in general when using unbiased value estimates, and in particular when using TD-learning—the predominant learning approach—under general assumptions. This enables practical trade-offs under the same resource constraints, such as the use of smaller memory to enable larger policy networks and the use of partial—instead of full—observations for better generalisation.

3. Empirical analysis: We run several experiments in a variety of T-maze tasks—a canonical memory benchmark—using standard RL algorithms like Q-learning and PPO. Results demonstrate that AS generally leads to better memory management and sample efficiency than FS with κ memory (when k^* is unknown), while having comparable sample efficiency to FS with k^* memory (when k^* is given by an oracle).

2 Problem Setting

The Environment. We are interested in non-Markovian environments, which can be modelled as a Non-Markovian Decision Process (NMDP). Here, an agent interacts in an environment receiving observations $x_t \in \mathcal{X}$ at each step $t \in \{0, 1, \dots, T\}$ and producing action $a_t \in \mathcal{A}$, where T is the length of an episode (or the lifetime of the agent in non-episodic settings). The agent’s action causes the environment to transition to a new observation $x_{t+1} \in \mathcal{X}$ and also provides the agent with a scalar reward $r_{t+1} \in \mathbb{R}$. The environment is k^* -order Markovian (i.e. a k^* -order Markov Decision Process (Puterman, 2014)), meaning that $k^* \in \mathbb{N}$ is the smallest number such that the probability function $Pr(x_{t+1}, r_{t+1}|x_{t:t-k^*}, a_t)$ is stationary regardless of the agent’s policy, where $x_{t:t-k^*}$ includes the last k^* observations.² If $k^* = 1$, then this is a standard Markov Decision Processes (MDP). We are interested in designing realistic computationally limited agents that can perform in environments where k^* is very large. Note that our setting closely mirrors that of partially observable Markov decision processes (POMDP) (Kaelbling et al., 1998) where the last k^* observations constitute a sufficient statistic of the state of the environment. In our work, discussion of the environment state is not necessary as we make no attempt to build a formal belief state as is commonly done in POMDPs. The notion of a memory state that we focus on building can be far more compact at scale.

The Agent. The agent acts in the environment using a policy $\pi(a_t|x_{t:t-k^*})$, which can be characterised by a value function $V^\pi(x_{t:t-k^*}) := \mathbb{E}_{a_t \sim \pi, (x_{t+1}, r_{t+1}) \sim Pr} [\sum_{t=0}^{\infty} \gamma^t r_{t+1} | x_{t:t-k^*}]$. The agent’s objective is to learn an optimal policy π^* that maximizes their long-term accumulated reward, characterised by the optimal value function $V^*(x_{t:t-k^*}) = \max_\pi V^\pi(x_{t:t-k^*})$. However, the agent must learn π^* with finite computational resources including a working memory w (i.e. RAM) of finite capacity (in bits) $|w| \leq |w|^*$, and computational resources c of finite capacity (in allowable floating point operations per environment step) $|c| \leq |c|^*$ split across both inference and learning. The size and architecture of the agents parameters θ must be chosen such that the two resource limits are always respected. Most recent progress in AI has been driven by sequence models (e.g. Transformers or RNNs), which in our setting would learn a policy of the form $\pi_\theta(a_t|x_{t:t-k})$. A fully differentiable sequence model has at least a linear dependence with respect to the sequence length k of the working memory size $|w| \in \Omega(k)$ and computation $|c| \in \Omega(k)$ (for both inference and learning). For the popular Transformer architecture, it is actually even worse $|c| \in \Omega(k^2)$.

The Problem. For a fully differentiable sequence model to learn in environments with large k^* , we must then correspondingly decrease the model size $|\theta|$ so that we can accommodate for the agent’s limitations in terms of working memory $|w|^*$ and computational resources $|c|^*$. However, in many environments with high k^* , only $\kappa \ll k^*$ observations are actually needed to predict the environment dynamics. Thus k^* is only large because the relevant observations are spaced apart by long temporal distances, not because there are many relevant observations to consider. So then if we learn to maintain a memory of size $k^* \geq k \geq \kappa$ with RL, we can improve the efficiency of computation and working memory by a factor of $\Omega(k^*/\kappa)$ and increase $|\theta|$ at the same resource budget. Additionally, such an abstraction will induce a search space reduction by a factor of $\mathcal{O}(|\mathcal{X}|^{k^*-\kappa})$, which could

²For clarity and without loss of generality, we only consider the history of observations and not the history of actions and rewards, since these can always be included in the agents observations.

lead to improvements in sample efficiency and generalisation for a policy using it. In this work, we consider approaches for achieving this goal with deep sequence models.

3 Adaptive Stacking

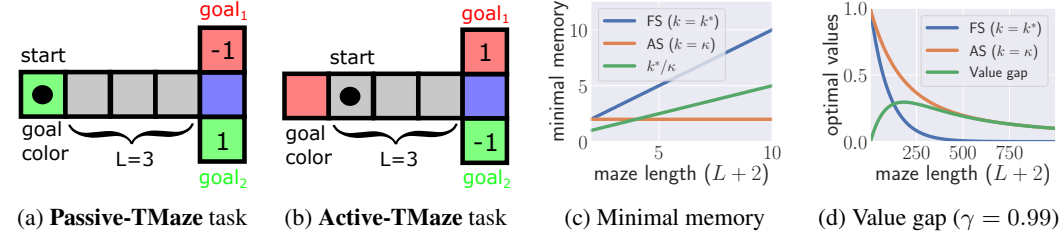


Figure 2: **TMaze** environment. There are only 4 observations here, corresponding to the color of the grid cell the agent is in: *red* \blacksquare for $goal_1$, *green* \blacksquare for $goal_2$, *blue* \blacksquare for the maze junction, and *grey* \blacksquare for the maze corridor. The given goal (red or green sampled uniformly) is only shown at the tail end of the maze, and the corridor has length L . The agent is represented by the black dot and has four cardinal actions for navigation. (a) **Passive-TMaze** task. The agent starts at the tail end of the maze. It then takes one step to the right at every time step regardless of its action, until the junction location where the top and right actions achieve $goal_1$ while the down and left actions achieve $goal_2$. (b) **Active-TMaze** task. The agent starts one step to the right of the tail end of the maze. It then moves in the cardinal direction corresponding to its action at every time step, or stays still if the action hits the maze walls—for example taking the up or down actions in the corridor and the right action at the junction. (c) Minimal memory stack required when using Frame Stacking vs Adaptive Stacking in the Passive-TMaze. (b) The *value gap* between the optimal values (using Frame Stacking with $k = k^* = L + 2$), and the perceived optimal values (using Adaptive Stacking with $k = \kappa = 2$) when an agent has observed \blacksquare then \blacksquare under their respective optimal policies in the Passive-TMaze. The perceived optimal values under an optimal policy is higher than the true optimal values because of uncertainty over the environment history (Section 3.2).

We propose *Adaptive Stacking* as a general-purpose memory abstraction for reinforcement learning in partially observable environments. Adaptive Stacking extends the common frame stacking heuristic by endowing the agent with control over which past observations to retain in a bounded memory stack of size k . Rather than passively retaining the most recent k observations, the agent *actively decides* which observation to discard—which could be the current observation. This transforms memory management into a decision-making problem aligned with maximizing reward.

Motivating Examples. Consider the TMaze environment illustrated in Figure 2, a canonical memory task from neuroscience (O’Keefe & Dostrovsky, 1971) which we adapt similarly to prior benchmark works (Bakker, 2001; Osband et al., 2019; Hung et al., 2019; Ni et al., 2023): 1. **Passive-TMaze task (Figure 2a):** Here, the agent only needs to remember the goal cue in order to pick the correct goal at the junction cue, and doesn’t need to learn to navigate in the maze (hence $k^* = L + 2$). Frame Stacking, due to its FIFO nature, forgets the goal signal when the maze is longer than the memory window ($k < L + 2$). In contrast, with an adaptive stacking approach, the agent can learn to retain the goal-defining observation across time and discard irrelevant grey observations—thereby solving the task with a much smaller memory budget. 2. **Active-TMaze task (Figure 2b):** Here, the agent must both navigate to find the goal color and remember it to navigate to the corresponding goal location. Hence $k^* = \infty$ since a non-optimal policy can stay arbitrarily long in the grey corridor, making the environment non-stationary unless the whole history is kept in memory. An adaptive stacking approach can learn to discard irrelevant movement observations while retaining the goal cue across time, mimicking selective attention and long-term binding found in biological agents.

3.1 RL with Internal Memory Decisions

Formally, Adaptive Stacking induces a new decision process where the agent at each timestep t receives an observation $x_t \in \mathcal{X}$ and maintains a memory stack $s_t = [x_{i_1}, x_{i_2}, \dots, x_{i_k}]$ containing k selected past observations indexed by their timesteps. We will refer to this memory stack as the *agent state* (Dong et al., 2022). Upon receiving x_{t+1} , the agent must execute two actions: an *environment action* $a_t \in \mathcal{A}$ (e.g., move left or right), and a *memory action* $i_t \in \{1, \dots, k\}$ selecting which memory element to pop. The agent state is then updated as: $s_{t+1} = \text{push}(\text{pop}(s_t, i_t), x_{t+1})$.

In general, this process induces a new POMDP $\mathcal{M}_k = \langle \mathcal{M}, \mathcal{S}, \mathcal{I}, u \rangle$ where \mathcal{M} is the original POMDP, \mathcal{S} is the set of agent states, \mathcal{I} is the set of *memory management actions*, and $u : \mathcal{S} \times \mathcal{I} \times \mathcal{X} \rightarrow \mathcal{S}$ is a *memory update function* (such as the *push-pop* stack update). The agent’s policy is now $\pi_k(a_t, i_t | s_t)$, which can be characterised by a perceived value function $V_k^{\pi_k}(s_t) := \mathbb{E}_{(a_t, i_t) \sim \pi_k, (x_{t+1}, r_{t+1}) \sim Pr} [\sum_{t=0}^{\infty} \gamma^t r_{t+1} | u(s_t, i_t, x_{t+1})]$ that represents the agent’s perceived values. Its objective is now to learn an optimal policy π_k^* that maximizes its long-term accumulated reward, characterised by the perceived optimal value function $V_k^*(s_t) = \max_{\pi_k} V_k^{\pi_k}(s_t)$ that represents the agent’s perceived optimal values. We show how to instantiate this process in Algorithm 1 using Q-learning, but the approach is applicable to any RL algorithm. Importantly, the approach is also compatible with modern architectures such as Transformers by simply defining \mathcal{S} , \mathcal{I} , and u appropriately—leading to compute and memory benefits as described in the Appendix. By integrating the memory update into the RL loop (see Figure 1), Adaptive Stacking fits cleanly into existing learning pipelines and can be trained end-to-end.

In this view, Adaptive Stacking transforms memory selection into a sequential decision-making problem aligned with the agent’s reward signal. This stands in contrast to passive memory mechanisms based on Frame Stacking, which indiscriminately process all inputs. This also aligns with cognitive models of working memory in humans, where attention-gated memory buffers retain only task-relevant cues while filtering distractors (Unger et al., 2016). However, this raises an important question: How does selective forgetting affect the standard theoretical guarantees established for the convergence RL agents—such as value function and policy optimality?

3.2 Value Preserving Optimality

While Adaptive Stacking is designed to learn which past observations to retain, a key theoretical question is how this compression affects the ability of RL agents to preserve optimal behaviour. Specifically, we want to understand how the perceived value function under Adaptive Stacking relates to the true value function under full-history policies. We first observe that there is a general relationship between the adaptive stack perceived value function and the underlying full-history value function: $V_k^{\pi_k}(s_t) = \sum_{x_{t:t-k^*}} Pr(x_{t:t-k^*} | s_t, \pi_k) V^{\pi_k}(x_{t:t-k^*})$ for all $s_t \in \mathcal{S}$, where $Pr(x_{t:t-k^*} | s_t, \pi_k)$ is the asymptotic probability amortized over time that the environment k^* -history is $x_{t:t-k^*}$ when the agent state is s_t under policy π_k (Singh et al., 1994). This equation shows that the agent’s perceived value under compressed memory is an expectation over possible latent histories. When the memory stack discards critical observations, this conditional distribution becomes broader, increasing uncertainty. However, this loss in value does not necessarily imply a suboptimal policy.

To see this, consider the Passive-TMaze example with corridor length $L = 3$, so that $k^* = L + 2 = 5$. Suppose the agent uses an Adaptive Stacking policy with memory size $k = 2$. The optimal adaptive policy π_2^* , illustrated in Figure 5, learns to retain only the green goal indicator and discard irrelevant grey observations. At timestep $t = 1$, the memory state is $s_t = \square \blacksquare \blacksquare$. However, multiple latent histories are compatible with this state: $x_{t:t-k^*} \in \{\square \blacksquare \blacksquare, \blacksquare \square \blacksquare, \blacksquare \blacksquare \square\}$. This gives:

$$V_2^{\pi_2^*}(\square \blacksquare) = \frac{1}{3} V^{\pi_2^*}(\square \blacksquare \blacksquare) + \frac{1}{3} V^{\pi_2^*}(\blacksquare \square \blacksquare) + \frac{1}{3} V^{\pi_2^*}(\blacksquare \blacksquare \square) = \frac{1}{3}(\gamma^3 + \gamma^2 + \gamma).$$

However, the actual latent history at time $t = 1$ is $x_{t:t-k^*} = \square \blacksquare \blacksquare$, and the true optimal value is: $V^*(x_{t:t-k^*}) = \gamma^3$. This induces a value gap $|V^*(x_{t:t-k^*}) - V_2^{\pi_2^*}(s_t)| > 0$, but π_2^* is still optimal

since $V^{\pi_2^*}(x_{t:t-k^*}) = V^*(x_{t:t-k^*})$, even though s_t is not a sufficient statistic of the k^* -history $x_{t:t-k^*}$. Figure 2d shows the value gap for varying T-Maze lengths. This illustrates a crucial point:

Remark 1 *Uncertainty in history may harm value expectations, $|V^*(x_{t:t-k^*}) - V_k^{\pi_k^*}(s_t)| > 0$, but it does not necessarily harm policy optimality as long as the uncertain differences are irrelevant for optimal decision making: $V^*(x_{t:t-k^*}) = V^{\pi_k^*}(x_{t:t-k^*})$.*

In the TMaze example, discarding some grey cells does not affect the correct action at the junction, so the policy is optimal even if the perceived value is slightly pessimistic. This leads us to the following notion of a minimal sufficient memory length:

Definition 1 Define κ to be the smallest memory length such that there exists a policy π_κ^* satisfying $V^{\pi_\kappa^*}(x_{t:t-k^*}) = V^*(x_{t:t-k^*})$ for all t .

This characterises the minimal task-relevant context size needed to act optimally in environments with large k^* , and motivates the central promise of Adaptive Stacking: optimal memory management via reward-guided memory decisions. κ always exists since in the simplest case we can have $\kappa = k^*$ (Proposition 1), as shown in Figure 2c when the maze length is 2 (when $L = 0$). Hence, any unbiased RL algorithm that is guaranteed to converge to optimal policies under Frame Stacking with $k = k^*$ is also guaranteed to converge to optimal policies under Adaptive Stacking with $k = \kappa$ (Theorem 1).

Proposition 1 If $k = k^*$, then there exists a π_k^* such that $V^{\pi_k^*}(s_t) = V^*(x_{t:t-k^*})$ for all $s_t \in \mathcal{S}$.

Theorem 1 Let \mathbb{A} be an RL algorithm that converges under Frame Stacking with $k \geq k^*$. If \mathbb{A} uses unbiased value estimates to learn optimal policies, then it also converges under Adaptive Stacking with $k \geq \kappa$ observations, assuming the policy class is sufficiently expressive.

Hence, an agent can use unbiased RL algorithms such as REINFORCE to learn optimal Adaptive Stacking policies (provided the value estimates are also convex). However, such algorithms often suffer from large variance (Sutton & Barto, 2018). To address this, we also provide convergence guarantees using TD-learning in Appendix C.4, which is used by state-of-the-art algorithms like PPO (Schulman et al., 2017). This shows that an agent does not need to be able to predict states nor disambiguate trajectories to learn useful value estimates. When the memory length k is sufficiently large ($k \geq \kappa$), this ensures convergence to an optimal policy despite non-Markovian dynamics. This has significant implications for compute and memory efficiency when using sequence models like Transformers. Transformers incur compute costs of $\Omega(k^2)$ and working memory costs of $\Omega(k)$ due to self-attention over long contexts (Narayanan et al., 2021; Anthony et al., 2023). Adaptive Stacking reduces these to $\Omega(\kappa^2)$ and $\Omega(\kappa)$ respectively, by retaining only reward-relevant observations of length $\kappa \ll k^*$ —thereby yielding substantial efficiency gains in both inference and training shown in Table 4. See Appendix I for derivations.

4 Experiments

We evaluate Adaptive Stacking on variants of the T-Maze task (Figure 2) to assess both learning performance and memory management. We compare against two baselines: FrameStack with $k = \kappa$ (insufficient memory) and $k = k^*$ (oracle memory)³, and report three metrics: (1) **Rewards regret**: difference in achieved values between the optimal and learn policies, (2) **Memory regret**: number of steps when the goal cue is absent from the memory stack (excluding the top of the stack which corresponds to the current observation), and (3) **Returns**: cumulative discounted rewards. All error bars represent one standard deviation across a number of random seeds (N_{rs}).

³In the active maze, k^* is infinite since a non-optimal policy could stay arbitrarily long in the grey corridor. Hence, Frame Stacking with $k = k^* = \infty$ is unable learn in the continual active maze since there are no environment resets (and hence memory resets), violating the assumption of infinite exploration needed for most algorithms (like Q-learning). Given this, we instead use $k = L + 2$ for this experiment.

Continual TMaze with Q-learning. We first evaluate in a continual Passive-TMaze and Active-TMaze, where episodes do not terminate, and rewards are only given at goal transitions. This stresses the agent’s ability to persist and discard information appropriately. Results (Figures 3 and 4) show that Adaptive Stacking achieves high returns and low reward regret, consistent with theoretical predictions. When $\kappa = k^*$, all methods perform similarly. But when $\kappa < k^*$, AS retains significantly lower memory regret than $FS(\kappa)$, learning to preserve goal cues over long delays. Note that $FS(k^*)$, even in the Passive-Tmaze, still incurs some memory regret since the top of the stack is not used for this metric.

Architecture-agnostic performance. To evaluate whether Adaptive Stacking depends on a specific sequence model, we compare returns across MLP, LSTM, and Transformer policies using PPO in the Passive-TMaze (Figure 1 right). In this experiment, the task is episodic with variable corridor lengths ($L \in [0, 14]$) per episode. We observe consistent relative performance: AS significantly outperforms FS with $k = \kappa$ and achieves comparable training returns to the oracle $FS(k^*)$ baseline, regardless of architecture. This highlights that our approach is architecture-agnostic and complements various model classes, including attention- and recurrence-based policies. See the Appendix for learning curves and additional results using MLPs, LSTMs and Transformers.

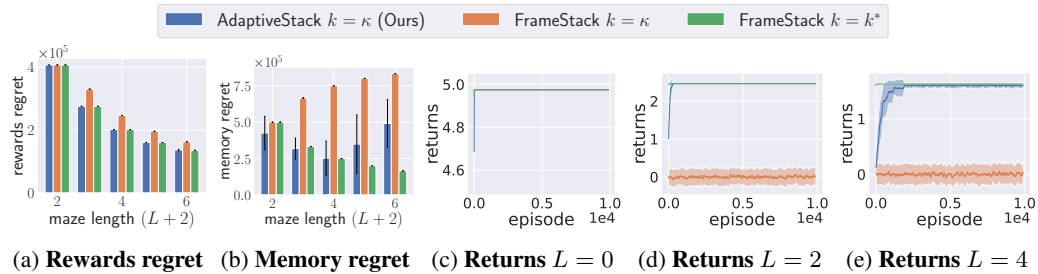


Figure 3: Continual **Passive-TMaze** with Q-learning ($N_{rs} = 20$). AS matches the oracle $FS(k^*)$ in returns and memory usage, while outperforming $FS(\kappa)$ especially for long-term dependencies.

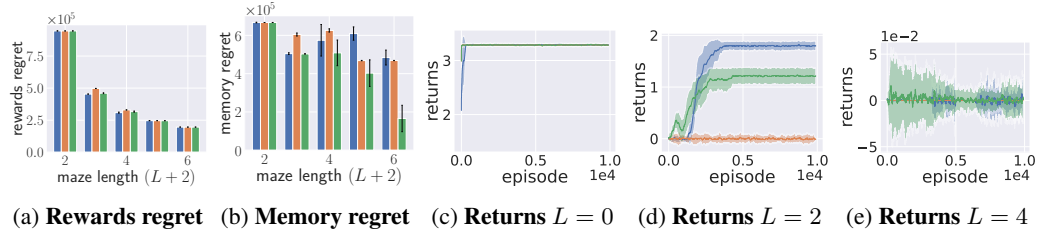


Figure 4: Continual **Active-TMaze** with Q-learning ($N_{rs} = 20$). AS learns to both recall and discard task-relevant observations, achieving near-oracle returns with lower memory regret than $FS(\kappa)$.

5 Conclusion

We have introduced **Adaptive Stacking**, a general-purpose meta-algorithm for learning to manage memory in partially observable environments. Unlike standard frame stacking, which blindly retains recent observations, Adaptive Stacking allows agents to learn which observations to remember or discard via reinforcement learning. We showed that this yields theoretical guarantees on policy optimality under both unbiased optimization and TD-based learning, even when using a significantly smaller memory than required for full observability. Experiments across multiple TMaze tasks confirm that Adaptive Stacking matches the performance of oracle memory agents while using far less memory, and substantially outperforms naive baselines under tight memory budgets. This offers a promising path toward scalable, memory-efficient RL in large, partially observable environments.

6 Broader Impacts

We propose a general-purpose method for improving memory efficiency in reinforcement learning. On the positive side, this could broaden access to advanced RL systems by reducing their computational and memory demands, which is especially beneficial in low-resource settings such as education, mobile robotics, and emerging economies. It may also enhance agent interpretability by encouraging sparse and task-relevant memory use. On the negative side, more memory-efficient agents could be more easily deployed in surveillance or autonomous systems with limited oversight, potentially increasing the risk of misuse or unintended harm. Furthermore, optimising for memory efficiency may lead to implicit biases in what the agent chooses to remember or forget. Future work should explore safeguards for memory gating decisions, particularly in safety-critical domains.

References

- David Abel, Will Dabney, Anna Harutyunyan, Mark K Ho, Michael Littman, Doina Precup, and Satinder Singh. On the expressivity of markov reward. *Advances in Neural Information Processing Systems*, 34:7799–7812, 2021.
- David Abel, André Barreto, Hado van Hasselt, Benjamin Van Roy, Doina Precup, and Satinder Singh. On the convergence of bounded agents. *arXiv preprint arXiv:2307.11044*, 2023.
- Cameron Allen, Aaron Kirtland, Ruo Yu Tao, Sam Lobel, Daniel Scott, Nicholas Petrocelli, Omer Gottesman, Ronald Parr, Michael Littman, and George Konidaris. Mitigating partial observability in sequential decision processes via the lambda discrepancy. *Advances in Neural Information Processing Systems*, 37:62988–63028, 2024.
- Quentin Anthony, Stella Biderman, and Hailey Schoelkopf. Transformer math 101, 2023.
- Kai Arulkumaran, Marc Peter Deisenroth, Miles Brundage, and Anil Anthony Bharath. Deep reinforcement learning: A brief survey. *IEEE Signal Processing Magazine*, 34(6):26–38, 2017.
- Bram Bakker. Reinforcement learning with long short-term memory. *Advances in neural information processing systems*, 14, 2001.
- Jacob Beck, Kamil Ciosek, Sam Devlin, Sebastian Tschiatschek, Cheng Zhang, and Katja Hofmann. Amrl: Aggregated memory for reinforcement learning. In *International Conference on Learning Representations*, 2020.
- Tristan Bester, Benjamin Rosman, Steven James, and Geraud Nangue Tasse. Counting reward automata: Sample efficient reinforcement learning through the exploitation of reward function structure. *arXiv preprint arXiv:2312.11364*, 2023.
- Yuji Cao, Huan Zhao, Yuheng Cheng, Ting Shu, Yue Chen, Guolong Liu, Gaoqi Liang, Junhua Zhao, Jinyue Yan, and Yun Li. Survey on large language model-enhanced reinforcement learning: Concept, taxonomy, and methods. *IEEE Transactions on Neural Networks and Learning Systems*, 2024.
- Lili Chen, Kevin Lu, Aravind Rajeswaran, Kimin Lee, Aditya Grover, Misha Laskin, Pieter Abbeel, Aravind Srinivas, and Igor Mordatch. Decision transformer: Reinforcement learning via sequence modeling. *Advances in neural information processing systems*, 34:15084–15097, 2021.
- Maxime Chevalier-Boisvert, Lucas Willems, and Suman Pal. Minimalistic gridworld environment for openai gym. <https://github.com/maximecb/gym-minigrid>, 2018. GitHub repository.
- Shi Dong, Benjamin Van Roy, and Zhengyuan Zhou. Simple agent, complex environment: Efficient reinforcement learning with agent states. *Journal of Machine Learning Research*, 23(255):1–54, 2022.

- Max Esslinger et al. Memory gym: A benchmark for long-term memory in reinforcement learning. In *Advances in Neural Information Processing Systems*, volume 35, pp. 12345–12356, 2022.
- Meire Fortunato et al. Psychlab: A psychology laboratory for deep reinforcement learning agents. In *Advances in Neural Information Processing Systems*, volume 32, pp. 1637–1648, 2019.
- Karl Friston. The free-energy principle: a rough guide to the brain? *Trends in cognitive sciences*, 13(7):293–301, 2009.
- Yunfan Gao, Yun Xiong, Xinyu Gao, Kangxiang Jia, Jinliu Pan, Yuxi Bi, Yixin Dai, Jiawei Sun, Haofen Wang, and Haofen Wang. Retrieval-augmented generation for large language models: A survey. *arXiv preprint arXiv:2312.10997*, 2:1, 2023.
- Anirudh Goyal, Abram Friesen, Andrea Banino, Theophane Weber, Nan Rosemary Ke, Adria Puigdomenech Badia, Arthur Guez, Mehdi Mirza, Peter C Humphreys, Ksenia Konyushova, et al. Retrieval-augmented reinforcement learning. In *International Conference on Machine Learning*, pp. 7740–7765. PMLR, 2022.
- Alex Graves, Greg Wayne, and Ivo Danihelka. Neural turing machines. *arXiv preprint arXiv:1410.5401*, 2014.
- Albert Gu, Karan Goel, and Christopher Ré. Efficiently modeling long sequences with structured state spaces. *arXiv preprint arXiv:2111.00396*, 2021.
- Hosein Hasanbeig, Natasha Yogananda Jeppu, Alessandro Abate, Tom Melham, and Daniel Kroening. Symbolic task inference in deep reinforcement learning. *Journal of Artificial Intelligence Research*, 80:1099–1137, 2024.
- Matthew J Hausknecht and Peter Stone. Deep recurrent q-learning for partially observable mdps. In *AAAI fall symposia*, volume 45, pp. 141, 2015.
- Sepp Hochreiter and Jürgen Schmidhuber. Long short-term memory. *Neural computation*, 9(8):1735–1780, 1997.
- Chia-Chun Hung, Timothy Lillicrap, Josh Abramson, Yan Wu, Mehdi Mirza, Federico Carnevale, Arun Ahuja, and Greg Wayne. Optimizing agent behavior over long time scales by transporting value. *Nature communications*, 10(1):5223, 2019.
- Chia-Chun Hung et al. Optimizing agent behavior over long time scales by transporting value. In *International Conference on Machine Learning*, pp. 2043–2052, 2018.
- Rodrigo Toro Icarte, Toryn Klassen, Richard Valenzano, and Sheila McIlraith. Using reward machines for high-level task specification and decomposition in reinforcement learning. In *International Conference on Machine Learning*, pp. 2107–2116. PMLR, 2018.
- Rodrigo Toro Icarte, Toryn Q Klassen, Richard Valenzano, and Sheila A McIlraith. Reward machines: Exploiting reward function structure in reinforcement learning. *Journal of Artificial Intelligence Research*, 73:173–208, 2022.
- Khurram Javed and Richard S Sutton. The big world hypothesis and its ramifications for artificial intelligence. In *Finding the Frame: An RLC Workshop for Examining Conceptual Frameworks*, 2024.
- Khurram Javed, Haseeb Shah, Richard S Sutton, and Martha White. Scalable real-time recurrent learning using columnar-constructive networks. *Journal of Machine Learning Research*, 24(256):1–34, 2023.
- Khurram Javed, Arsalan Sharifnassab, and Richard S Sutton. Swifttd: A fast and robust algorithm for temporal difference learning. In *Reinforcement Learning Conference*, 2024.

Leslie Pack Kaelbling, Michael L Littman, and Anthony R Cassandra. Planning and acting in partially observable stochastic domains. *Artificial intelligence*, 101(1-2):99–134, 1998.

Merlijn Krale, Thiago D Simao, and Nils Jansen. Act-then-measure: reinforcement learning for partially observable environments with active measuring. In *Proceedings of the International Conference on Automated Planning and Scheduling*, volume 33, pp. 212–220, 2023.

Andrew Lampinen et al. Towards mental time travel: A hierarchical memory for reinforcement learning agents. *arXiv preprint arXiv:2112.08369*, 2021.

Patrick Lewis, Ethan Perez, Aleksandra Piktus, Fabio Petroni, Vladimir Karpukhin, Naman Goyal, Heinrich Küttler, Mike Lewis, Wen-tau Yih, Tim Rocktäschel, et al. Retrieval-augmented generation for knowledge-intensive nlp tasks. *Advances in neural information processing systems*, 33: 9459–9474, 2020.

Volodymyr Mnih, Koray Kavukcuoglu, David Silver, Alex Graves, Ioannis Antonoglou, Daan Wierstra, and Martin Riedmiller. Playing atari with deep reinforcement learning. *arXiv preprint arXiv:1312.5602*, 2013.

Steven Morad, Ryan Kortvelesy, Matteo Bettini, Stephan Liwicki, and Amanda Prorok. Popgym: Benchmarking partially observable reinforcement learning. *arXiv preprint arXiv:2303.01859*, 2023.

Deepak Narayanan, Mohammad Shoeybi, Jared Casper, Patrick LeGresley, Mostafa Patwary, Vijay Korthikanti, Dmitri Vainbrand, Prethvi Kashinkunti, Julie Bernauer, Bryan Catanzaro, et al. Efficient large-scale language model training on gpu clusters using megatron-lm. In *Proceedings of the International Conference for High Performance Computing, Networking, Storage and Analysis*, pp. 1–15, 2021.

Tianwei Ni, Benjamin Eysenbach, and Ruslan Salakhutdinov. Recurrent model-free rl can be a strong baseline for many pomdps. *arXiv preprint arXiv:2110.05038*, 2021.

Tianwei Ni, Michel Ma, Benjamin Eysenbach, and Pierre-Luc Bacon. When do transformers shine in rl? decoupling memory from credit assignment. *Advances in Neural Information Processing Systems*, 36:50429–50452, 2023.

John O’Keefe and Jonathan Dostrovsky. The hippocampus as a spatial map: preliminary evidence from unit activity in the freely-moving rat. *Brain research*, 1971.

Ian Osband, Yotam Doron, Matteo Hessel, John Aslanides, Eren Sezener, Andre Saraiva, Katrina McKinney, Tor Lattimore, Csaba Szepesvari, Satinder Singh, et al. Behaviour suite for reinforcement learning. *arXiv preprint arXiv:1908.03568*, 2019.

Ian Osband et al. Behaviour suite for reinforcement learning. In *International Conference on Learning Representations*, 2020.

Emilio Parisotto and Ruslan Salakhutdinov. Neural map: Structured memory for deep reinforcement learning. *arXiv preprint arXiv:1702.08360*, 2017.

Emilio Parisotto, Francis Song, Jack Rae, Razvan Pascanu, Caglar Gulcehre, Siddhant Jayakumar, Max Jaderberg, Raphael Lopez Kaufman, Aidan Clark, Seb Noury, et al. Stabilizing transformers for reinforcement learning. In *International conference on machine learning*, pp. 7487–7498. PMLR, 2020.

Vytas Pasukonis et al. Evaluating long-term memory in 3d mazes. *arXiv preprint arXiv:2210.13383*, 2022.

Marco Pleines et al. Memory gym: Partially observable challenges to memory-based agents. In *International Conference on Learning Representations*, 2023.

- Martin L Puterman. *Markov decision processes: discrete stochastic dynamic programming*. John Wiley & Sons, 2014.
- Herbert Robbins and Sutton Monro. A stochastic approximation method. *The annals of mathematical statistics*, pp. 400–407, 1951.
- Noor Sajid, Philip J Ball, Thomas Parr, and Karl J Friston. Active inference: demystified and compared. *Neural computation*, 33(3):674–712, 2021.
- Mohammad Reza Samsami, Artem Zholus, Janarthanan Rajendran, and Sarath Chandar. Mastering memory tasks with world models. *arXiv preprint arXiv:2403.04253*, 2024.
- John Schulman, Filip Wolski, Prafulla Dhariwal, Alec Radford, and Oleg Klimov. Proximal policy optimization algorithms. *arXiv preprint arXiv:1707.06347*, 2017.
- Satinder P Singh, Tommi Jaakkola, and Michael I Jordan. Learning without state-estimation in partially observable markovian decision processes. In *Machine Learning Proceedings 1994*, pp. 284–292. Elsevier, 1994.
- Richard S Sutton and Andrew G Barto. *Reinforcement learning: An introduction*. MIT press, 2018.
- Erik Talvitie and Satinder Singh. Learning to make predictions in partially observable environments without a generative model. *Journal of Artificial Intelligence Research*, 42:353–392, 2011.
- Geraud Nangue Tasse, Devon Jarvis, Steven James, and Benjamin Rosman. Skill machines: Temporal logic skill composition in reinforcement learning. 2024.
- Rodrigo Toro Icarte, Ethan Waldie, Toryn Klassen, Rick Valenzano, Margarita Castro, and Sheila McIlraith. Learning reward machines for partially observable reinforcement learning. *Advances in neural information processing systems*, 32, 2019.
- Kerstin Unger, Laura Ackerman, Christopher H Chatham, Dima Amso, and David Badre. Working memory gating mechanisms explain developmental change in rule-guided behavior. *Cognition*, 155:8–22, 2016.
- Pashootan Vaezipoor, Andrew C Li, Rodrigo A Toro Icarte, and Sheila A Mcilraith. Ltl2action: Generalizing ltl instructions for multi-task rl. In *International Conference on Machine Learning*, pp. 10497–10508. PMLR, 2021.
- Ashish Vaswani, Noam Shazeer, Niki Parmar, Jakob Uszkoreit, Llion Jones, Aidan N Gomez, Łukasz Kaiser, and Illia Polosukhin. Attention is all you need. *Advances in neural information processing systems*, 30, 2017.
- Fan Yang and Phu Nguyen. Recurrent world models facilitate policy evolution. In *Advances in Neural Information Processing Systems*, volume 34, pp. 1009–1021, 2021.

Supplementary Materials

The following content was not necessarily subject to peer review.

A Related Work

While the classical RL framework assumes a Markov Decision Process (MDP), a large number of real-world decision-making problems such as meta-learning, robust RL, temporal credit assignment, and generalization, are naturally cast as POMDPs (Ni et al., 2021; 2023). These tasks often require reasoning over long histories of observations rather than relying solely on current state information, necessitating agents with memory or other mechanisms for long-term temporal inference.

Agents without working memory. Foundational work has shown that settings that violate the Markov property introduce substantial complexity. For example, Singh et al. (1994) and Talvitie & Singh (2011) demonstrated that applying standard TD-learning in POMDPs leads to biased value estimates. Given this, Singh et al. (1994) proposed stochastic policies over observations to obtain higher returns compared to deterministic policies, and Talvitie & Singh (2011) introduced prediction profile models—non-generative models focusing on predicting only task-relevant events. More fundamentally, Abel et al. (2021) proved that there exist tasks whose optimal behavior cannot be induced by any Markovian reward function. Consequently, these tasks are not just more difficult, but fundamentally non-Markovian demanding memory for optimal performance. Classical solutions attempt to address this problem by maintaining a belief state (distribution over states) as a sufficient statistic of the history (Kaelbling et al., 1998; Friston, 2009; Sajid et al., 2021). However, exact belief-state planning is intractable for complex environments, so modern RL agents rely on learned memory or state representations to approximate the hidden state without full state estimation.

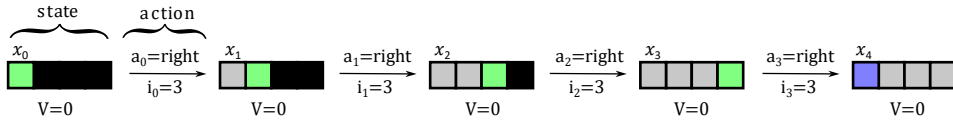
Agents with sequence models. A common practical solution to partial observability is *Frame Stacking*—concatenating the most recent k observations to form a proxy for the state (Mnih et al., 2013). While effective in environments with short temporal dependencies (such as Atari), FS scales poorly with the memory horizon: increasing k exponentially expands the input space. To address this, recurrent neural networks (RNNs) such as Long Short Term Memories (LSTMs) and Gated Recurrent Units (GRUs) have been employed (Hausknecht & Stone, 2015), offering a learned internal state representation. Yet, these architectures often struggle in long-horizon tasks due to gradient vanishing, limited capacity, and sensitivity to training dynamics (Singh et al., 1994; Ni et al., 2021). Recent improvements such as Javed et al. (2023; 2024) have focused on better RNNs training methods (like real-time recurrent learning) and temporal difference estimation methods like SwiftTD to improve the learning speed and stability of online RL. In a separate line of works, Transformers have been increasingly applied to RL settings—inspired by their success in natural language processing (NLP) (Vaswani et al., 2017). Self-attention allows these models to learn to focus on relevant past events and scale to longer memory horizons. Parisotto et al. (2020) proposed GTrXL, demonstrating improved stability over LSTMs. Chen et al. (2021) introduced the Decision Transformer, a sequence model for offline RL. Most relevant to this work, Ni et al. (2023) rigorously studied the separation of memory length and credit assignment. They showed that Transformers can remember cues over a relatively large number of steps in synthetic T-Maze tasks, but struggle with long-term credit assignment. These works still depend on maintaining a memory stack of length k^* using FS to learn optimal policies.

Agents agnostic to sequence models. Several works attempt to bypass the exponential blow-up in agent states by learning compact, predictive memory representations for arbitrary sequence models. Allen et al. (2024) introduced λ -*discrepancy*, a measure of the deviation between TD targets with and without bootstrapping. They prove that this discrepancy is zero in fully observed MDPs and positive in POMDPs, offering a diagnostic and learning signal for memory sufficiency. Alternative strategies include learning which observations are worth remembering. Most closely related to our work is the *Act-Then-Measure* framework (Krale et al., 2023), which lets agents actively choose when to

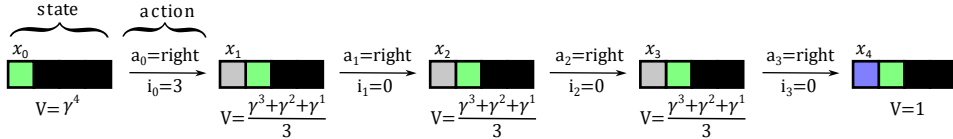
observe their state, balancing the cost of memory against its value. However, these works still use Frame Stacking when the stack is full, and hence can be seamlessly integrated with learning-based memory selection methods such as our Adaptive Stacking method. Finally, Abel et al. (2023) recently considers bounded agents in general—agents with finite memory or computational resources—and provide frameworks for understanding convergence in this setting.

Agents with episodic memory. Beyond recurrence and attention, researchers have developed more explicit neural memory systems to handle partial observability. These include external memory modules and learned differentiable storage that the agent can read and write to. For instance, Graves et al. (2014) introduced the Neural Turing Machine, which augments a neural network with an addressable memory matrix. Such architectures can, in principle, be used in RL to memorize arbitrarily long sequences (Graves et al., 2014). Similarly, (Parisotto & Salakhutdinov, 2017) proposed the Neural Map, a 2D structured memory for agents to store and retrieve information over long navigation trajectories. Memory-augmented agents, including those with differentiable neural dictionaries or key-value memory banks such as retrieval augmented generations (RAGs), have shown the ability to recall events much later in an episode than traditional networks (Lewis et al., 2020; Gao et al., 2023; Goyal et al., 2022). These approaches demonstrate that more sophisticated memory mechanisms can improve an agent’s performance in environments requiring long-term information retention (Osband et al., 2019; Morad et al., 2023), although they often come with increased complexity, training difficulty, and require disk space memory. Hence, these works can be combined with our adaptive stacking strategy to improve their use of working memory (RAM).

B Algorithms



(a) **Frame Stacking.** At every time step, the agent pops the last observation in the memory stack in order to free up space to push the new observation into the stack.



(b) **Adaptive Stacking.** At every time step, the agent chooses which observation in the memory stack to pop in order to free up space to push the new observation into the stack.

Figure 5: Illustration of Frame Stacking and Adaptive Stacking with $k = 4$ in the passive-TMaze with $k^* = L + 2 = 5$. Frame Stacking eventually forgets the goal trigger when the context length is not large enough ($k < k^*$), while Adaptive Stacking is able to remember the goal trigger by choosing to forget irrelevant grey observations. In this figure, ■ corresponds to an empty memory slot.

Algorithm 1: Q-Learning: Adaptive Stacking

Input : discounting $\gamma = 0.99$, learning rate $\alpha = 0.01$, exploration $\epsilon = 0$, memory length k

Initialise : value function $Q(s, \langle a, i \rangle) = R_{\text{MAX}}$

foreach *episode* **do**

 Get initial observation $x_0 \in \mathcal{X}$

 Initialise observation stack $s_0 \leftarrow [x_0]_k$ // e.g. $s_0 = [x_0, x_0]$ if $k = 2$

foreach timestep $t = 0, 1, \dots, T$ **while** *episode* **is not done** **do**

$$\langle a_t, i_t \rangle \leftarrow \begin{cases} \arg \max_{\langle a, i \rangle} Q(s_t, \langle a, i \rangle) & \text{w.p. } 1 - \epsilon \\ \text{a random action} & \text{w.p. } \epsilon \end{cases}$$

 Execute a_t , get reward r_{t+1} and next observation x_{t+1}

 Remove observation from stack $s_{t+1} \leftarrow \text{pop}(s_t, i_t)$

 Push observation into stack $s_{t+1} \leftarrow \text{push}(s_{t+1}, x_{t+1})$

$$Q(s_t, \langle a_t, i_t \rangle) \xleftarrow{\alpha} (r_{t+1} + \gamma \max_{\langle a, i \rangle} Q(s_{t+1}, \langle a, i \rangle)) - Q(s_t, \langle a_t, i_t \rangle)$$

C Theoretical Results

We begin by restating the key definitions and then give precise statements and proofs for our theoretical results.

C.1 Preliminaries and Notation

Let the underlying non-Markovian environment be a k^* -order MDP over observations $x_t \in \mathcal{X}$, with full-history value

$$V^*(x_{t:t-k^*}) = \max_{\pi} \mathbb{E} \left[\sum_{h=0}^{\infty} \gamma^h r_{t+h+1} \mid x_{t:t-k^*}, \pi \right].$$

Under Adaptive Stacking (AS) with memory size k , the agent memory state is $s_t = [x_{i_1}, \dots, x_{i_k}]$ and its value under policy π_k is

$$V_k^{\pi_k}(s_t) = \mathbb{E} \left[\sum_{h=0}^{\infty} \gamma^h r_{t+h+1} \mid s_t, \pi_k \right] = \sum_{x_{t:t-k^*}} \Pr(x_{t:t-k^*} \mid s_t, \pi_k) V^{\pi_k}(x_{t:t-k^*}), \quad (1)$$

where $V^{\pi_k}(x_{t:t-k^*})$ is the full-history value of π_k using Frame Stacking (FS).

We define

$$\kappa = \min \{k \in \mathbb{N} : \exists \pi_k^* \text{ with } V_k^{\pi_k^*}(x_{t:t-k^*}) = V^*(x_{t:t-k^*}) \forall t\}.$$

C.2 Proof of Proposition 1

Proposition 1 If $k = k^*$, then there exists a policy π_k^* such that $V_k^{\pi_k^*}(s_t) = V^*(x_{t:t-k^*})$ for all t .

Proof When $k = k^*$, the Adaptive Stacking agent can simply retain the last k^* observations in order, equivalently to Frame Stacking. Thus, no important information is discarded, and the agent can follow an optimal full-history policy π_k^* on $s_t = [x_t, x_{t-1}, \dots, x_{t-k^*}]$. Hence,

$$\Pr(x_{t:t-k^*} \mid s_t, \pi_k^*) = \begin{cases} 1 & \text{if } s_t = x_{t:t-k^*}, \\ 0 & \text{otherwise,} \end{cases}$$

implying $V_k^{\pi_k^*}(s_t) = V^{\pi_k^*}(s_t) = V^{\pi_k^*}(x_{t:t-k^*}) = V^*(x_{t:t-k^*})$. ■

C.3 Proof for Theorem 1

Theorem 1 in the main paper stated that traditional RL algorithms that converge under Frame Stacking with $k \geq k^*$ also converge under Adaptive Stacking, provided they use unbiased value estimates to learn optimal policies. We first formally state this unbiased convergence assumption:

Assumption C.1 (Unbiased Convergence) *Let \mathbb{A} be an RL algorithm that converges under Frame Stacking with $k \geq k^*$. Assume that for any memory length $k \in \mathbb{N}$, \mathbb{A} also converges to a k -order policy*

$$\pi_k^*(x_{t:t-k}) = \arg \max_{\pi_k} \hat{V}^{\pi_k}(x_{t:t-k}) \quad \forall t,$$

where $\hat{V}^{\pi_k}(x_{t:t-k})$ is an unbiased estimator of the true return:

$$\mathbb{E} [\hat{V}^{\pi_k}(x_{t:t-k})] = V^{\pi_k}(x_{t:t-k}).$$

We now restate the result more formally and provide a detailed proof.

Theorem 1 *Let \mathbb{A} be an RL algorithm that satisfies Assumption C.1. Then for any $k \geq \kappa$, \mathbb{A} converges to an optimal Adaptive Stacking policy π_k^* such that:*

$$V^{\pi_k^*}(x_{t:t-k^*}) = \max_{\pi} V^{\pi}(x_{t:t-k^*}) \quad \forall t.$$

Proof Adaptive Stacking with memory size k induces a new decision process \mathcal{M}_k in which the agent new observation is the memory state $s_t \in \mathcal{S}_k$, a stack of k underlying environment observations. This process can be treated as a POMDP, where the true underlying state is the latent history $x_{t:t-k^*}$.

By definition of κ , there exists at least one k -order policy π_k with $k \geq \kappa$ that achieves the optimal value on all underlying latent histories:

$$V^{\pi_k}(x_{t:t-k^*}) = V^*(x_{t:t-k^*}) \quad \text{for all } t.$$

Since π_k acts on $s_t \in \mathcal{S}_k$ and implicitly induces a distribution over latent histories $x_{t:t-k^*}$, its value in the induced process is as shown in Equation 1. By construction of π_k , we have $V^{\pi_k}(x_{t:t-k^*}) = V^*(x_{t:t-k^*})$, so:

$$V_k^{\pi_k}(s_t) = \sum_{x_{t:t-k^*}} \Pr(x_{t:t-k^*} | s_t, \pi_k) V^*(x_{t:t-k^*}) = \mathbb{E}_{x_{t:t-k^*}} [V^*(x_{t:t-k^*}) | s_t].$$

This implies that the policy π_k achieves the best possible value in the induced process \mathcal{M}_k given that it is optimal over latent histories.

Now, because \mathbb{A} uses unbiased estimates of $V^{\pi_k}(x_{t:t-k})$ and converges to the policy that maximizes expected return under such estimates (by Assumption C.1), and since $k \geq \kappa$ implies such a policy exists, it follows that \mathbb{A} converges to π_k^* that satisfies:

$$V^{\pi_k^*}(x_{t:t-k^*}) = V^*(x_{t:t-k^*}) \quad \forall t.$$

■

The critical observation from Theorem 1 is that convergence to an optimal policy is not limited to $k \geq k^*$, but to any $k \geq \kappa$, where κ is the minimal sufficient memory required to disambiguate value-relevant latent histories. The key assumption for this result is that \mathbb{A} optimizes return estimates that are unbiased *with respect to the true value under the full history*, for example as achieved by Monte Carlo policy gradient methods like REINFORCE (Sutton & Barto, 2018).

We emphasize that this result does not extend to TD-based methods (which use biased targets), and is handled separately in Section C.4.

C.4 Proof for TD-Learning convergence

We now prove that if two policies have an ordering over value functions in the induced memory POMDP \mathcal{M}_k , and the memory representation is value-consistent, then the same ordering holds over the original latent histories.

Assumption C.2 (Value-Consistency) *Let π_k be an Adaptive Stacking policy over memory states $s_t \in \mathcal{S}_k$. We say the memory representation is value-consistent with respect to π_k if for any $s_t \in \mathcal{S}_k$ and any two latent histories $x_{t:t-k^*}, x'_{t:t-k^*}$ such that*

$$\Pr(x_{t:t-k^*} | s_t, \pi_k) > 0 \quad \text{and} \quad \Pr(x'_{t:t-k^*} | s_t, \pi_k) > 0,$$

it holds that:

$$V^{\pi_k}(x_{t:t-k^*}) = V^{\pi_k}(x'_{t:t-k^*}).$$

Theorem 2 (Partial-order Preserving) *Let $k \in \mathbb{N}$ and let π_k^1, π_k^2 be two policies under Adaptive Stacking such that for all memory states $s_t \in \mathcal{S}_k$:*

$$V_k^{\pi_k^1}(s_t) \leq V_k^{\pi_k^2}(s_t).$$

If both policies induce value-consistent memory representations (Assumption C.2), then for all latent histories $x_{t:t-k^*}$:

$$V^{\pi_k^1}(x_{t:t-k^*}) \leq V^{\pi_k^2}(x_{t:t-k^*}).$$

Proof By Equation 1, the expected return under π_k^1 in the induced memory process is:

$$V_k^{\pi_k^1}(s_t) = \sum_{x_{t:t-k^*}} \Pr(x_{t:t-k^*} | s_t, \pi_k^1) V^{\pi_k^1}(x_{t:t-k^*}).$$

Under Assumption C.2, for each $i \in \{1, 2\}$, all latent histories $x_{t:t-k^*}$ consistent with a memory state s_t have equal value:

$$V^{\pi_k^i}(x_{t:t-k^*}) = c_i(s_t), \quad \text{a constant.}$$

Hence, the above expectation reduces to:

$$V_k^{\pi_k^1}(s_t) = c_1(s_t).$$

Therefore, the ordering assumption implies:

$$c_1(s_t) = V^{\pi_k^1}(x_{t:t-k^*}) \leq V^{\pi_k^2}(x_{t:t-k^*}) = c_2(s_t),$$

for all $x_{t:t-k^*}$ such that $\Pr(x_{t:t-k^*} | s_t, \pi_k^1) > 0$.

Thus, the partial ordering $V_k^{\pi_k^1}(s_t) \leq V_k^{\pi_k^2}(s_t)$ implies:

$$V^{\pi_k^1}(x_{t:t-k^*}) \leq V^{\pi_k^2}(x_{t:t-k^*}) \quad \text{for all } x_{t:t-k^*}. \quad \blacksquare$$

We now prove that Temporal Difference (TD) learning converges to the optimal policy under Adaptive Stacking, provided that $k \geq \kappa$ and the memory representation is value-consistent.

Theorem 3 *Let $k \geq \kappa$, and suppose Q-learning under standard learning assumptions (Robbins & Monro, 1951) is applied to the induced decision process \mathcal{M}_k under a fixed exploratory policy that ensures persistent exploration. If policies in \mathcal{M}_k are value-consistent, then:*

1. The Q -function $Q(s, a, i)$ converges with probability 1 to a fixed point $\hat{Q}(s, a, i)$.
2. The greedy policy with respect to \hat{Q} is optimal. That is, $\pi_k^*(s_t) \in \arg \max_{(a,i)} \hat{Q}(s_t, a, i)$ achieves the optimal value $V^*(x_{t:t-k^*})$.

Proof Since the agent operates over the induced process \mathcal{M}_k , its effective state is $s_t \in \mathcal{S}_k$. The Q-learning update rule is:

$$Q_{t+1}(s_t, a_t, i_t) \leftarrow Q_t(s_t, a_t, i_t) + \alpha_t \left[r_{t+1} + \gamma \max_{(a',i')} Q_t(s_{t+1}, a', i') - Q_t(s_t, a_t, i_t) \right],$$

where $s_{t+1} = \text{push}(\text{pop}(s_t, i_t), x_{t+1})$ is the updated memory stack, and α_t is a learning rate satisfying the standard conditions:

$$\sum_t \alpha_t = \infty, \quad \sum_t \alpha_t^2 < \infty.$$

Under the assumption that all (s, a, i) tuples are visited infinitely often, and rewards are bounded, Theorem 2 of [Singh et al. \(1994\)](#) guarantees that $Q(s, a, i)$ converges to the fixed point $\hat{Q}(s, a, i)$.

Since $k \geq \kappa$, by definition of κ , there exists a policy π_k^* such that for all latent histories $x_{t:t-k^*}$:

$$V^{\pi_k^*}(x_{t:t-k^*}) = V^*(x_{t:t-k^*}).$$

Because memory length k is sufficient to represent all task-relevant distinctions (the disambiguation required for value prediction), we know from Theorem 2 that under the value-consistency assumption, the policy π_k^* that is greedy with respect to \hat{Q} in the induced process \mathcal{M}_k will also be optimal in the underlying latent space:

$$\pi_k^*(s_t) \in \arg \max_{(a,i)} \hat{Q}(s_t, a, i) \quad \Rightarrow \quad V^{\pi_k^*}(x_{t:t-k^*}) = V^*(x_{t:t-k^*}) \quad \forall t.$$

Thus, Q-learning in the adaptive stacking process not only converges, but yields an optimal policy over the original environment when $k \geq \kappa$. \blacksquare

D Value-Consistency Assumption in Popular Benchmarks

In this section, we analyze common RL benchmarks to determine when our Value-Consistency (VC) Assumption C.2 holds. Recall that this assumption requires that all full histories $x_{t:t-k^*}$ mapping to the same agent memory state s_t under policy π_k must share the same expected return $V^{\pi_k}(x_{t:t-k^*})$. This often holds in goal-reaching or sparse-reward settings, but can be violated in tasks with dense or history-sensitive rewards (such as unobservable reward machines).

Table 1 summarizes our analysis, and we provide justification for each task below.

T-Maze (Classic) ([Bakker, 2001](#)): The agent observes a goal cue at the start, traverses a corridor, and makes a binary decision at a junction. Here, $k^* = T = 70$, since full observability only comes from the initial and final steps. However, $\kappa = 2$ suffices: the initial cue and position are enough to act optimally. VC holds since all consistent histories that lead to the same stack (for example, seeing “green”) yield the same value.

TMaze Long ([Beck et al., 2020](#)): Structurally identical to Classic T-Maze but with longer horizon $T = 100$. Again, $k^* = T$, $\kappa = 2$, and VC holds for the same reason.

Reacher-POMDP ([Yang & Nguyen, 2021](#)): The goal is revealed only at the first step, so k^* must capture that first observation. Any policy only needs to retain that goal and act accordingly, so $\kappa = 2$ suffices. VC holds since differing histories that preserve the same goal state will yield the same value estimate.

Task	T	k^*	κ	Assumption C.2 (VC) Holds?
T-Maze (Classic) (Bakker, 2001)	70	70	2	✓: Only goal cue matters
TMaze Long (Beck et al., 2020)	100	100	2	✓: Only goal cue matters
Reacher-POMDP (Ni et al., 2021)	50	Long	2	✓: Only goal cue matters
PyBullet-P (Ni et al., 2021)	1000	2	2	✓: Only previous position matters
HeavenHell (Esslinger et al., 2022)	20	T	2	✓: Only goal cue matters
PsychLab (Fortunato et al., 2019)	600	T	Long	✓: Passive episodic recall
Repeat First (Morad et al., 2023)	832	2	2	✓: Only previous optimal action matters
Passive Visual Match (Hung et al., 2018)	600	T	Long	✓: Only goal cue and apples affects return
MiniGrid-Memory (Chevalier-Boisvert et al., 2018)	1445	≤ 51	2	✓: Position suffices after goal cue
Memory Cards (Esslinger et al., 2022)	50	2	Long	✓: Only current card pairs affect rewards
Memory Length (Osband et al., 2020)	100	T	2	✓: Observation i.i.d. per timestep
Memory Maze (Pasukonis et al., 2022)	4000	Long	Long	✓: Only current transition affect rewards
Ballet (Lampinen et al., 2021)	1024	≥ 464	≥ 464	✓: Rewards unaffected by previous actions
Mortar Mayhem (Pleines et al., 2023)	135	T	T	✓: Rewards unaffected by previous actions
Autoencode (Morad et al., 2023)	312	312	156	✓: Rewards unaffected by previous actions
Numpad (Parisotto et al., 2020)	500	T	N^2	✓: Rewards unaffected by previous actions
Reward Machines (Icarte et al., 2022)	1000	T	T	✗: Rewards affected by previous actions
Passive T-Maze (Episodic) (Ours)	64	64	2	✓: Only goal cue matters
Passive T-Maze (Continual) (Ours)	10^6	64	2	✓: Only goal cue matters
Active T-Maze (Episodic) (Ours)	100	∞	2	✓: Only goal cue matters
Active T-Maze (Continual) (Ours)	10^6	∞	2	✓: Only goal cue matters

Table 1: Evaluation of Value-Consistency (VC) assumption across popular RL benchmark tasks. T is the maximum episode horizon or total training steps (for continual settings). k^* is the memory length required to make the environment Markov; Long means a relatively large proportion of the episode must be remembered to make optimal value predictions. κ is the minimal memory length required to achieve optimal return. Finally, VC Holds states whether Value-Consistency is satisfied.

PyBullet-P (Ni et al., 2021): This environment occludes the velocity component, but full observability is achieved after two steps (position and estimated velocity). Thus, $k^* = 2 = \kappa$. VC holds as only immediate transitions affect return.

HeavenHell (Esslinger et al., 2022): The agent visits an oracle early in the episode which defines the correct terminal target. The memory requirement is $k^* = T = 20$, but once the cue is retained, $\kappa = 2$ ensures optimality. VC holds because different paths to the same cue yield identical future returns.

PsychLab (Fortunato et al., 2019): Involves passive image memorization, typically from the beginning of an episode. $k^* = T = 600$, but memorizing the image is sufficient ($\kappa = \text{Long}$). VC holds due to deterministic mapping from memory state to return.

Repeat First (Morad et al., 2023): Rewards depend on repeating the first action. $k^* = T$, but $\kappa = 2$ suffices by retaining just the first action. VC holds since the memory state is value-determining.

Passive Visual Match (Hung et al., 2018): The goal color is observed passively at the start. The main reward depends only on whether the agent chooses the matching color at the end (plus intermediate rewards from collecting apples). $k^* = T = 600$, but $\kappa = T$. VC holds since the goal cue and nearby apples fully determines return.

MiniGrid-Memory (Chevalier-Boisvert et al., 2018): To plan efficiently, the agent must memorize a cue seen early and traverse a grid. The worst-case $k^* \leq 51$ and $\kappa = 2$ for simple cue-based planning. VC holds because position and cue suffice. In practice, if the position is not given, it can be estimated using path intergration.

Memory Cards (Esslinger et al., 2022): The agent must match cards based on values seen in earlier steps. $k^* = 2$, but $\kappa = \text{Long}$ due to potential card permutations. VC holds because matching decisions are memory-conditional, not trajectory-sensitive.

Memory Length (Osband et al., 2020): Observations are i.i.d. at each step. $k^* = T = 100$, but optimality requires only $\kappa = 2$. VC holds since memory state compresses all relevant statistics.

Memory Maze (Pasukonis et al., 2022): Agent must collect colored balls in order. The reward depends only on the current pickup. $k^* = \text{Long}$, $\kappa = \text{Long}$. VC holds since rewards depend only on present state and target.

Ballet (Lampinen et al., 2021): Agent observes sequences of dances and selects a correct dancer. Though the reward is episodic, the agent actions occur only post-observation. $k^* \geq 464$, $\kappa \geq 464$. VC holds because the same memory state determines the post-dance plan.

Mortar Mayhem (Pleines et al., 2023): Memorizing a command sequence and executing it. $k^* = T = 135$, $\kappa = T$. VC holds due to value depending solely on correctly recalling the command sequence.

Autoencode (Morad et al., 2023): Agent reproduces observed sequence in reverse. $k^* = 311$, $\kappa = 156$ (half the trajectory). VC holds since the value depends only on accuracy of reproduction.

Numpad (Parisotto et al., 2020): Agent must press a sequence of pads. $k^* = T = 500$, $\kappa = N^2$. VC holds: as long as the memory contains the correct order, the actual transition path is irrelevant.

Our Passive and Active T-Maze (in Episodic and Continual settings): In all our TMaze variants, the goal cue is shown at the tail of the maze and the return depends only on whether the goal is

reached. k^* matches the maze traversal length for the Passive-TMaze, but is infinite for the active maze since a non-optimal policy could stay arbitrarily long in the grey corridor, and $\kappa = 2$. VC holds robustly, even under stochastic start states or corridor lengths.

D.1 Unobservable Reward Machines Counter-Example

While the Value-Consistency Assumption holds in many benchmark settings (Table 1), it fails in environments where the true reward function depends not just on environment observations, but on dynamic latent trajectory properties such as event sequences which change based on the agent policy. This is most notably the case in environments that use *reward machines* (Icarte et al., 2018; Vaezi poor et al., 2021; Icarte et al., 2022; Tasse et al., 2024)—finite state automata over temporal logic formulae that determine rewards or sub-goals based on the sequence of states visited.

For example, consider the task "*Deliver coffee to the office without breaking decorations*" in a the office grid-world environment (Icarte et al., 2022). The task is encoded as a reward machine over three atomic propositions: p_{coffee} (the agent visits the coffee location), p_{office} (the agent visits the office location), p_{decor} (the agent steps on any decoration tile). The agent starts at some initial location and must: visit the coffee location *first*, then visit the office location, without ever triggering p_{decor} . A reward of +1 is given only if the full trajectory satisfies the temporal formula:

$$(F(p_{\text{coffee}} \wedge X(Fp_{\text{office}}))) \wedge (G\neg p_{\text{decor}}).$$

Why VC Fails. In the native environment, the agent’s observations are just its (x, y) location—there is no explicit record of whether the coffee has been visited, or if a decoration tile was stepped on. Consequently, two different trajectories can lead to the same agent observation $s_t = (x, y)$ and memory stack $s_t = [x_{i_1}, \dots, x_{i_k}]$. Yet these trajectories may differ in *reward-relevant history*, for example, one might have stepped on a decoration earlier while another didn’t. Since the reward for reaching the office depends on whether the coffee was collected *and* no decorations were touched in the past—which is unobservable from s_t alone—the condition:

$$V^{\pi_k}(x_{t:t-k^*}) = V^{\pi_k}(x'_{t:t-k^*})$$

does *not* hold for histories $x_{t:t-k^*}, x'_{t:t-k^*}$ that lead to the same agent state s_t . Therefore, Assumption C.2 is violated. Other common temporal logic tasks that violate VC include:

- "*Collect key A before key B, then go to door*": reward depends on the *order* of events, not the final state.
- "*Don’t revisit any state*": any policy that loops violates the reward constraint, but the current memory may not capture visit counts.
- "*Eventually visit both goal zones A and B, but never touch lava*": again, whether lava was touched can be lost under memory compression.

The VC assumption breaks because environment-level memory states s_t are not sufficient statistics for the reward machine’s state. The true reward depends on a latent automaton state that evolves with trajectory-dependent triggers—this is equivalent to acting in a *cross-product MDP* over $(x, y) \times u$, where u is the internal automaton state.

Can the Failure Be Benign? Despite the theoretical violation, practical agents can still learn to behave correctly using Adaptive Stacking when: The reward machine state can be inferred from a small set of key observations; The agent learns to preserve these key triggers (for example, the first visit to coffee or decoration tiles); The failure to preserve value consistency leads to pessimistic value estimates, but not incorrect action selection.

Hence, reward machine tasks represent a natural and important class of environments where the VC assumption breaks due to latent trajectory-dependent semantics. This distinction is useful for future work aiming to blend Adaptive Stacking with automaton inference, or for delineating the boundaries of where value-consistent abstraction is theoretically sound.

E Experimental Details

All experiments use two variants of the T-Maze task (Passive and Active). In each variant, we consider both *continual* mode—where the agent steps automatically and episodes never terminate—and *episodic* mode—where the agent chooses navigation actions and an episode ends upon reaching a goal. Corridor lengths L vary from 2 up to 62. At each time step the agent receives a single categorical observation (cell color) and maintains a working memory of fixed size κ . We compare three memory management schemes:

1. **Adaptive stacking** of size κ , where at each step the agent chooses which slot to overwrite,
2. **Frame stacking** with $k = \kappa$ (insufficient) or $k = k^*$ (oracle).

All agents were implemented in PyTorch and Gymnasium. Tabular Q-learning used in-memory arrays, and PPO used Stable-Baselines3. Finally, all experiments were ran on CPU only Linux servers.

E.1 Recorded Metrics

Every 100 environment steps we log:

1. *Return*: cumulative discounted reward.
2. *Reward regret*: $V^*(x_{t:t-k^*}) - V^\pi(x_{t:t-k^*})$.
3. *Memory regret*: steps when the goal cue is absent from the memory stack, excluding the top of the stack which corresponds to the current observation.
4. *Active regret*: steps when the goal cue is observed but not stored.
5. *Passive regret*: steps when the goal cue is in memory but then discarded.

Plots report mean and 1 standard deviation over N_{rs} independent seeds.

E.2 Tabular Q-Learning (Continual and Episodic)

We run a standard ε -greedy tabular Q-learning agent in both Passive and Active T-Maze, under continual or episodic modes. Hyperparameters are listed in Table 2.

Table 2: Q-Learning hyperparameters

Parameter	Value
Discount factor γ	0.99
Learning rate α	0.1
Exploration ε	fixed 0.01
Total steps	10^6
Logging frequency	every 100 steps

E.3 Proximal Policy Optimization (Episodic and Continual)

We evaluate PPO with MLP, CNN, LSTM and Transformer policies in both Passive and Active T-Maze, under episodic or continual modes. Table 3 details the optimizer settings.

Each policy network receives the k -length memory stack as input and outputs two probability distributions: one over environment actions and one over memory-slot indices. The final policy is obtained by sampling each head independently.

MLP

1. *Input*: one-hot encoding of each of the k observations, concatenated into a vector.

Table 3: PPO hyperparameters

Parameter	Value
Total timesteps	10^6
Discount factor γ	0.99
GAE λ	0.95
Rollout length n_steps	128
Minibatch size	128
Epochs per update	10
Learning rate	3×10^{-4}
Clip range	0.2
Entropy coefficient	0.0 (default)
Value loss coefficient	0.5 (default)
Logging frequency	every 100 steps

2. *Hidden layers*: three fully-connected layers of 128 units.

3. *Outputs*:

- (a) **Env-action head**: linear layer to $|\mathcal{A}|$ logits.
- (b) **Memory-action head**: linear layer to k logits.

LSTM

- 1. *Input embedding*: each observation is embedded into a 128-dim vector.
- 2. *Sequence model*: single-layer LSTM with 128 hidden units processes the k embeddings.
- 3. *Readout*: final hidden state of size 128.
- 4. *Outputs*: two linear heads (as above) mapping the 128-dim readout to action logits.

Transformer

- 1. *Input embedding*: each observation is embedded into 128-dim, plus learned positional embeddings for positions $1, \dots, k$.
- 2. *Transformer decoder stack*: two layers, model dimension 128, 4 attention heads, feed-forward dimension 256.
- 3. *Readout*: the representation at the final time step.
- 4. *Outputs*: two linear heads mapping the 128-dim readout to environment logits and memory-slot logits.

F Learning Area Under the Curve Bar Plots

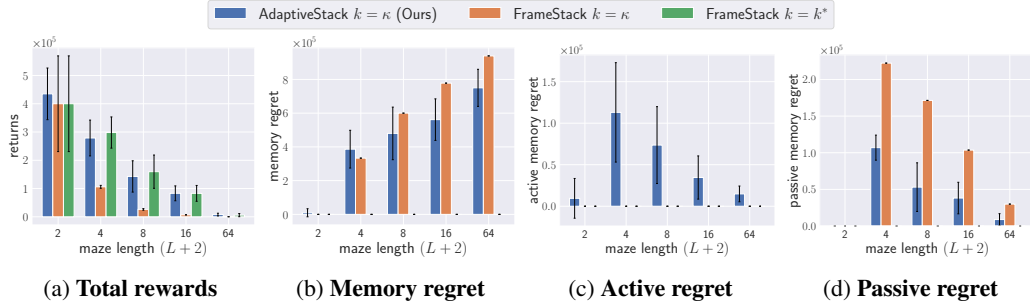


Figure 6: Episodic **Passive-TMaze** with PPO and LSTM policy ($N_{rs} = 10$). AS retains critical cues despite smaller memory, achieving performance close to $FS(k^*)$ and much better than $FS(\kappa)$.

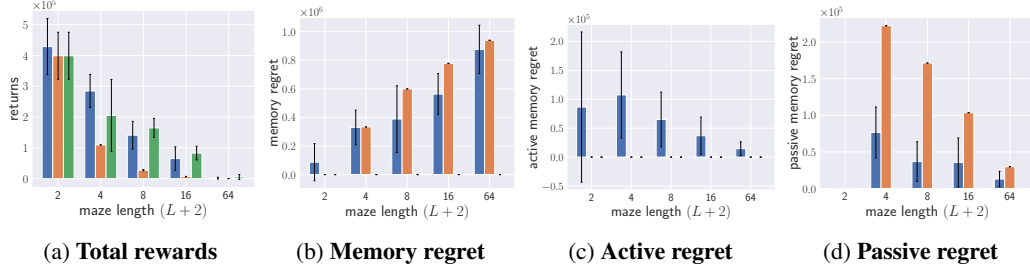


Figure 7: Episodic **Passive-TMaze** with PPO and Transformer policy ($N_{rs} = 10$). AS retains critical cues despite smaller memory, achieving performance close to $FS(k^*)$ and much better than $FS(\kappa)$.

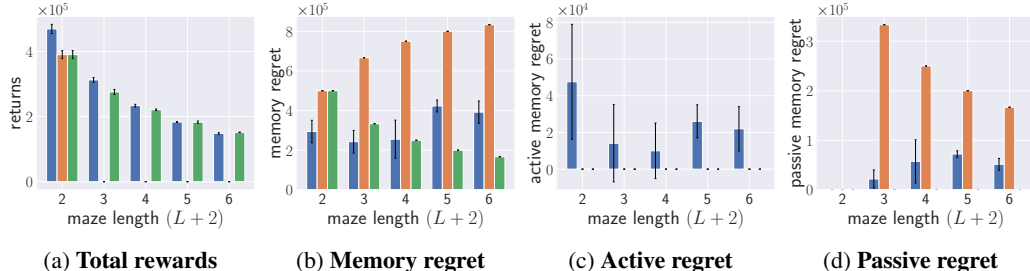


Figure 8: Episodic **Passive-TMaze** (with corridor lengths per episode fixed to max length) with PPO and MLP policy ($N_{rs} = 10$). AS retains critical cues despite smaller memory, achieving performance close to $FS(k^*)$ and much better than $FS(\kappa)$.

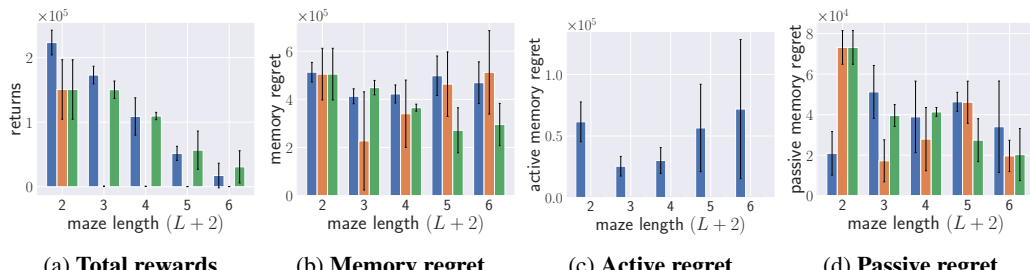


Figure 9: Episodic **Active-TMaze** (with corridor lengths per episode fixed to max length) with PPO and MLP policy ($N_{rs} = 10$). AS achieves performance close to $FS(k^*)$ and much better than $FS(\kappa)$.

G Learning Curves

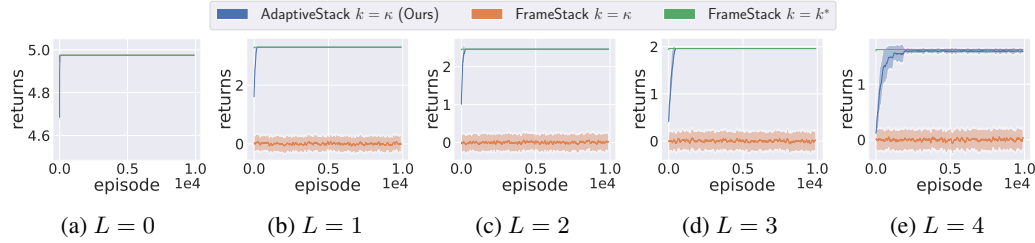


Figure 10: Returns in Continual **Passive-TMaze** with Q-learning ($N_{rs} = 20$) for varying maze lengths ($L + 2$). AS quickly matches the oracle FS(k^*) in returns, while outperforming FS(κ).

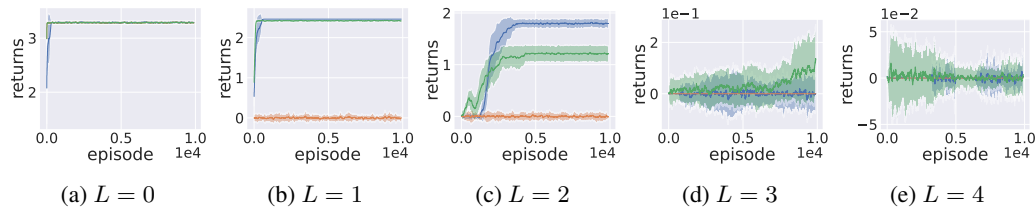


Figure 11: Returns in Continual **Active-TMaze** with Q-learning ($N_{rs} = 20$) for varying maze lengths ($L + 2$). AS quickly matches or exceeds the oracle FS(k^*) in returns, while outperforming FS(κ).

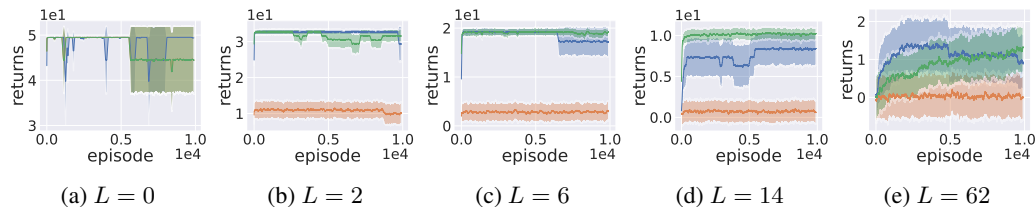


Figure 12: Returns in Episodic **Passive-TMaze** using PPO with an MLP ($N_{rs} = 10$) for varying maze lengths ($L + 2$). AS is comparable to the oracle FS(k^*) in returns, while outperforming FS(κ).

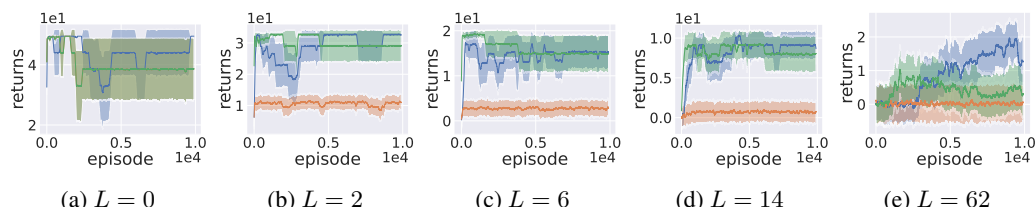


Figure 13: Returns in Episodic **Passive-TMaze** using PPO with an LSTM ($N_{rs} = 10$) for varying maze lengths ($L + 2$). AS is comparable to the oracle FS(k^*) in returns, while outperforming FS(κ).

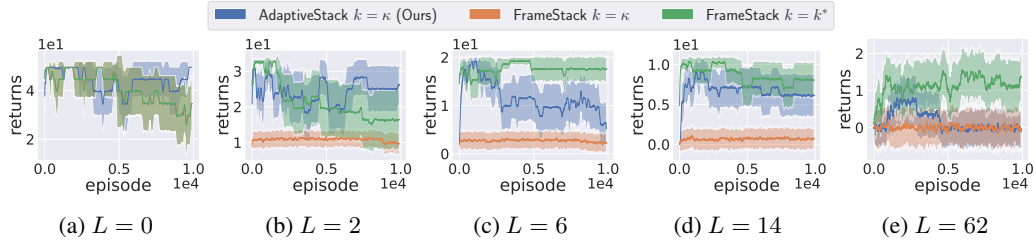


Figure 14: Returns in Episodic **Passive-TMaze** with PPO with an Transformer ($N_{rs} = 10$) for varying maze lengths ($L + 2$). AS matches the oracle $FS(k^*)$ in returns for smaller mazes but struggles to learn for larger mazes, while still outperforming $FS(\kappa)$, orange).

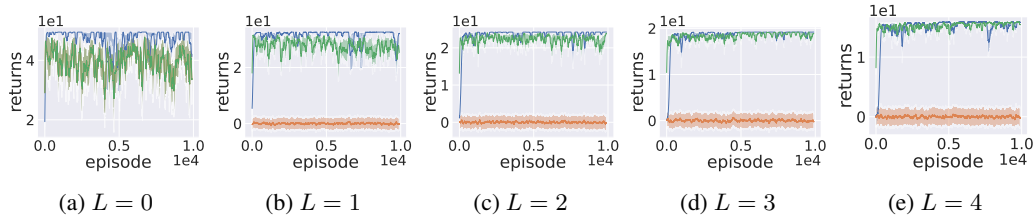


Figure 15: Returns in Episodic **Passive-TMaze** using PPO with an MLP ($N_{rs} = 10$) for varying maze lengths ($L + 2$). The corridor lengths per episode fixed to max length. AS quickly matches the oracle $FS(k^*)$ in returns, while outperforming $FS(\kappa)$, orange) especially for long-term dependencies.

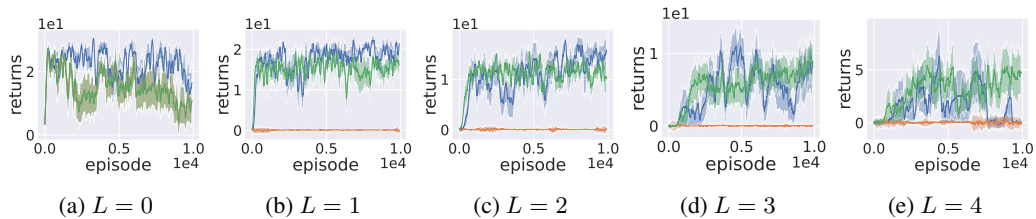


Figure 16: Returns in Episodic **Active-TMaze** with PPO with an MLP ($N_{rs} = 10$) for varying maze lengths ($L + 2$). The corridor lengths per episode fixed to max length. AS quickly matches the oracle $FS(k^*)$ in returns, while outperforming $FS(\kappa)$, orange).

H Evaluating Learned Policies

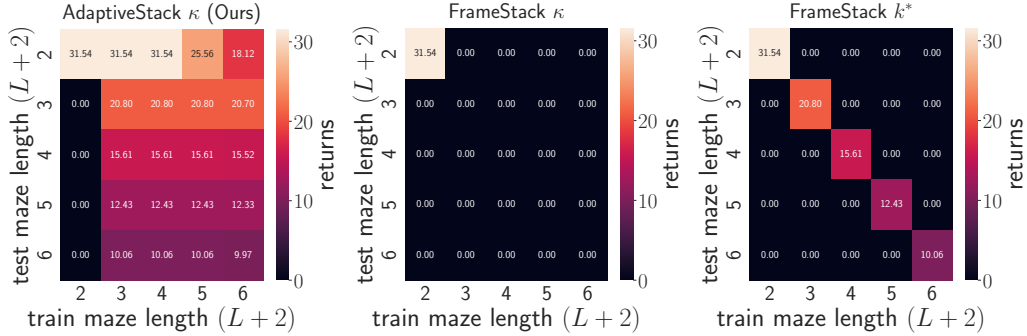


Figure 17: Generalisation in the continual **Passive-TMaze** with Q-learning ($N_{rs} = 20$). After training for 1 million steps, each agent is restarted at s_0 and tested for 100 additional steps in varying maze lengths. We show results averaged over the 20 training runs. We observe that AS leads to significantly better generalisation than FS(κ) and even the oracle FS(k^*).

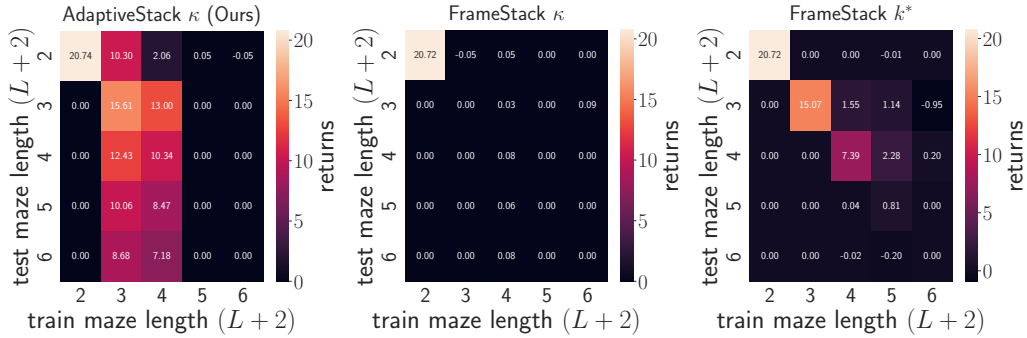


Figure 18: Generalisation in the continual **Active-TMaze** with Q-learning ($N_{rs} = 20$). AS still leads to significantly better generalisation than even using the oracle FS(k^*).

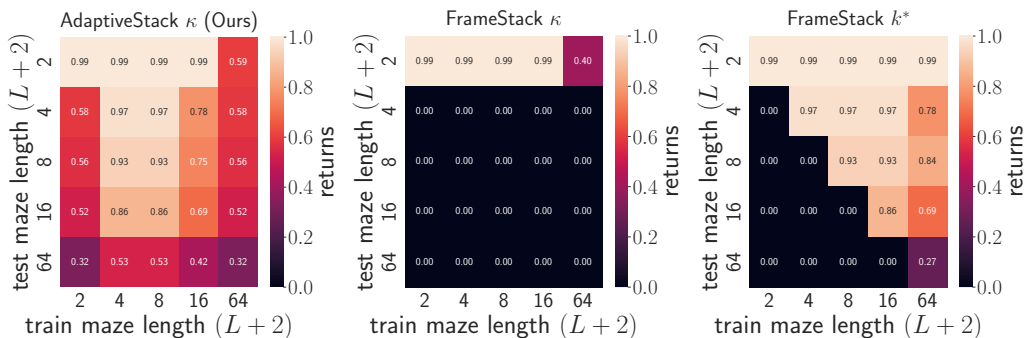


Figure 19: Generalisation in the episodic **Passive-TMaze** with PPO and MLP policy ($N_{rs} = 10$). After training for 1 million steps, each agent is tested for 2 additional episodes (for each goal color) in varying maze lengths (the corridor length in each testing episode is fixed to the max length). We show results averaged over the 10 training runs. We observe that the random corridor lengths during training leads to consistently good in-distribution generalisation (upper-diagonal), but AS still generally leads to better out-of-distribution generalisation (lower-diagonal) than even the oracle FS(k^*).

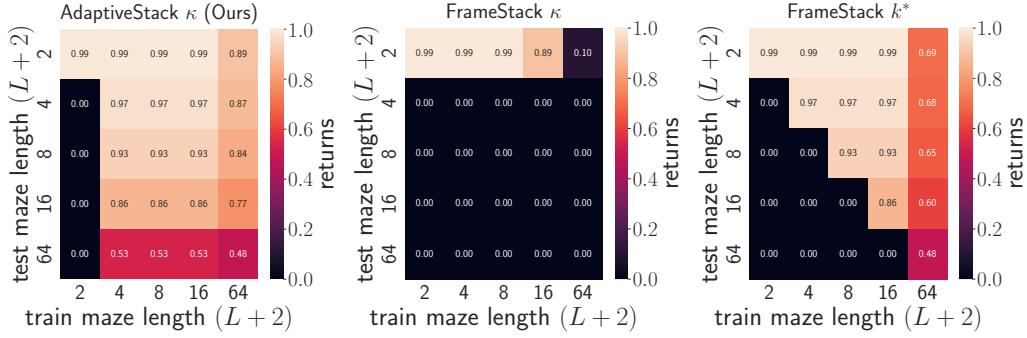


Figure 20: Generalisation in the episodic **Passive-TMaze** with PPO and LSTM policy ($N_{rs} = 10$). We observe similar results as Figure 19.

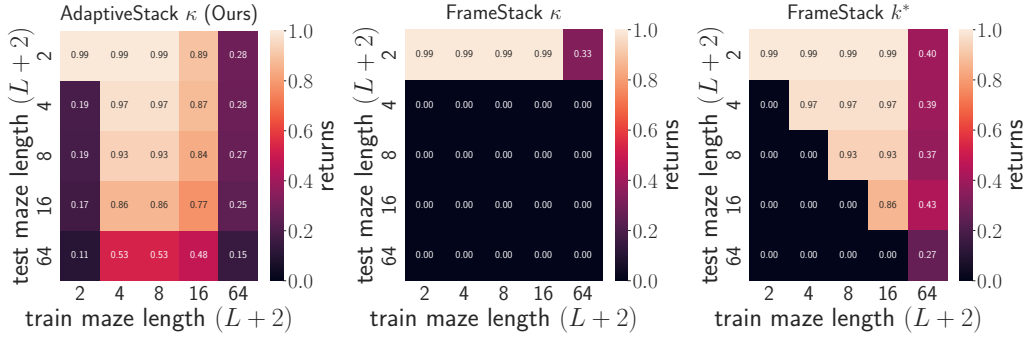


Figure 21: Generalisation in the episodic **Passive-TMaze** with PPO and Transformer policy ($N_{rs} = 10$). We observe similar results as Figure 19.

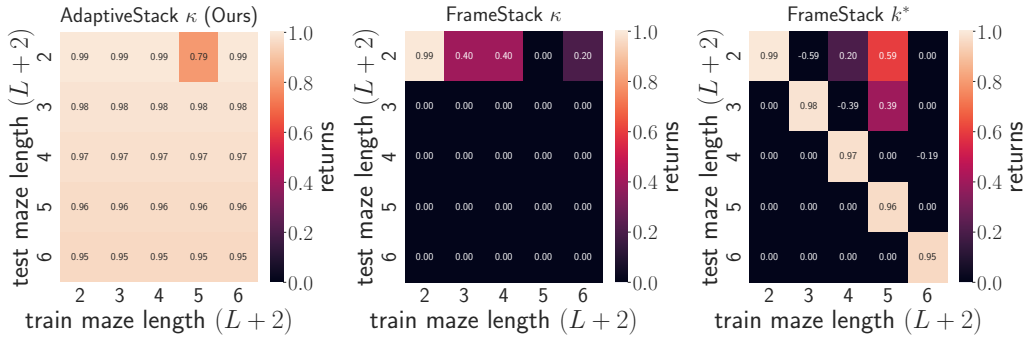


Figure 22: Generalisation in the episodic **Passive-TMaze** (with corridor lengths per episode fixed to max length) with PPO and MLP policy ($N_{rs} = 10$). We observe better results for AS and worse results for FS compared to Figure 19. This is potentially because AS generalises mainly from explicitly learning which observations to keep in memory, hence training with fixed corridor lengths simply leads to faster convergence. In contrast, FS mainly relies on the random corridor lengths during training to generalise.

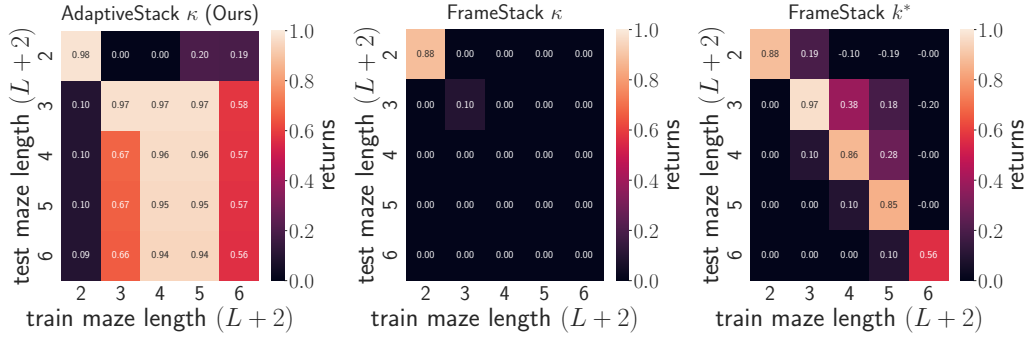


Figure 23: Generalisation in the episodic **Active-TMaze** (with corridor lengths per episode fixed to max length) with PPO and MLP policy ($N_{rs} = 10$). We observe similar results as Figure 22, except for maze lengths of 2. This difference is potentially because maze length 2 has no corridor (◻) observation, which makes it difficult to generalise the correct navigation actions to (and from) it.

I Compute and Memory Requirements for Transformers

In this section we analyse the compute and memory efficiency of Adaptive Stacking compared to Frame Stacking. We provide compute and memory requirements for MLP, LSTM, and Transformer models as a function of k , the context length processed by the model. In Table 1 of the main text, we further extend these results leveraging the fact that for Frame Stacking to learn the optimal policy $k \geq k^*$ and for Adaptive Stacking to learn the optimal policy $k \geq \kappa$.

I.1 MLP Models

Let us consider an MLP encoder model with weight precision \mathcal{P} bytes per unit, L layers, a hidden size of h , an action space size of $|\mathcal{A}|$, an inference batch size of $B_{\text{Inference}} = 1$, and a learning batch size of $B_{\text{Learn}} = B$. For uniformity with our analysis of the sequence models, we assume the input is already provided to the MLP in the form of k embeddings of size h , so the total input size is kh . We also assume a Relu non-linearity for each layer. Additionally, in the case of the Frame Stacking model, we assume that there is a linear output head with a value for each environment action in \mathcal{A} . Furthermore, in the case of the Adaptive Stacking model there is another linear output head with a value for each of the k memory eviction actions. The number of copies of the model G that needs to be stored in memory to compute updates during training depends on the learning optimizer. In the case of SGD, we only need to store a single gradient $G = 1$, whereas for the popular AdamW optimizer $G = 4$.

I.1.1 Producing a Single Action

Compute of Frame Stacking. In the first layer of the network $2kh^2 + h$ FLOPs are used for the linear layer due to the matrix multiplication and addition of bias (one multiply + one add per element of output). An additional h FLOPs are used for the Relu non-linearity computations. For the next $L - 1$ layers, $2h^2 + 2h$ FLOPs are used. In the final layer, $2h|\mathcal{A}|$ FLOPs are used. Therefore, the total FLOPs for a single action generation is:

$$|c|_{a \sim \pi_\theta} = 2kh^2 + 2h + (L - 1)(2h^2 + 2h) + 2h|\mathcal{A}| \in \Omega(k)$$

Compute of Adaptive Stacking. For Adaptive Stacking, we do the same amount of computation the first L layers of the network, one using the standard last layer with output size $|\mathcal{A}|$ and one using a layer of size k representing the memory action. This then brings the total FLOPs for a single action generation to:

$$|c|_{a \sim \pi_\theta} = 2kh^2 + 2h + (L - 1)(2h^2 + 2h) + 2h(|\mathcal{A}| + k) \in \Omega(k)$$

Memory of Frame Stacking. For MLP inference, we do not need to store intermediate activations after they are used. They are only needed when computing gradients. As such, we lower bound the memory needed for action inference by the number of parameters and precision of the model $|w|_{a \sim \pi_\theta} \geq \mathcal{P}|\theta|$ where $|\theta| = |\theta|_{\text{MLP}} + |\theta|_{\text{stack}}$. The weight matrix in the first layer has kh^2 parameters, the weight matrix in the middle $L - 1$ layers each have h^2 parameters, and the weight matrix in the last layers has $h|\mathcal{A}|$ parameters. The bias vector in the first L layers each have h parameters, and the bias vector in the last layer has $|\mathcal{A}|$ parameters. As such, the number of total number parameters is $|\theta|_{\text{MLP}} = kh^2 + (L - 1)h^2 + Lh + (h + 1)|\mathcal{A}|$. Additionally, the stack itself must store $|\theta|_{\text{stack}} = \mathcal{P}hk$. So the total RAM requirement of the model can be lower bounded as:

$$|w|_{a \sim \pi_\theta} \geq \mathcal{P}|\theta| = \mathcal{P}k(h^2 + h) + \mathcal{P}(L - 1)h^2 + \mathcal{P}Lh + \mathcal{P}(h + 1)|\mathcal{A}| \in \Omega(k)$$

Memory of Adaptive Stacking. The number of parameters in the Adaptive Stacking approach are the same for the first L layers, with the addition of a final layer with a weight matrix of size hk and a bias vector of size k . Additionally, the stack itself has the same number parameters as a function of k . So the total RAM requirement of the model can be lower bounded as:

$$|w|_{a \sim \pi_\theta} \geq \mathcal{P}|\theta| = \mathcal{P}k(h^2 + h) + \mathcal{P}(L - 1)h^2 + \mathcal{P}Lh + \mathcal{P}(h + 1)(|\mathcal{A}| + k) \in \Omega(k)$$

I.1.2 Producing a TD Update

Compute of Frame Stacking. To compute a TD update, we must perform two forward propagations for each item in the batch. The additional forward propagation is for computing the bootstrapping target using a target network that is the same size as the original network. The cost of a backward propagation should match that of a forward propagation, so it is clear that $|c|_{\text{TD}} = 3B|c|_{a \sim \pi_\theta}$. This then brings the total FLOPs for a TD batch update to:

$$|c|_{\text{TD}} = 3B \left(2kh^2 + 2h + (L - 1)(2h^2 + 2h) + 2h|\mathcal{A}| \right) \in \Omega(k)$$

Compute of Adaptive Stacking. In the case of Adaptive Stacking, we must perform TD updates for both the environment actions and the memory actions. Thus, we again have the relationship that $|c|_{\text{TD}} = 3B|c|_{a \sim \pi_\theta}$. This then implies that the total FLOPs for a TD batch update to:

$$|c|_{\text{TD}} = 3B \left(2kh^2 + 2h + (L - 1)(2h^2 + 2h) + 2h(|\mathcal{A}| + k) \right) \in \Omega(k)$$

Memory of Frame Stacking. During a TD update, we must also store the target network in memory, which has the same number of parameters as the original MLP. We also must store the activations of the main network now to compute the gradients. Thus, we can lower bound the memory required as $|w|_{\text{TD}} \geq (2 + G)\mathcal{P}|\theta|_{\text{MLP}} + \mathcal{P}B|\theta|_{\text{stack}} + \mathcal{P}BhL$, meaning the total RAM requirement of the model can be lower bounded as:

$$|w|_{\text{TD}} \geq (2 + G) \left(\mathcal{P}kh^2 + \mathcal{P}(L - 1)h^2 + \mathcal{P}Lh + \mathcal{P}(h + 1)|\mathcal{A}| \right) + \mathcal{P}Bkh + \mathcal{P}BhL \in \Omega(k)$$

Memory of Adaptive Stacking. We again have the fact that $|w|_{\text{TD}} \geq (2 + G)\mathcal{P}|\theta|_{\text{MLP}} + \mathcal{P}B|\theta|_{\text{stack}} + \mathcal{P}BhL$, but $|\theta|_{\text{MLP}}$ is different for Adaptive Stacking because of the extra final layer for the memory policy. So the total RAM requirement of the model can be lower bounded as:

$$|w|_{\text{TD}} \geq (2 + G) \left(\mathcal{P}kh^2 + \mathcal{P}(L - 1)h^2 + \mathcal{P}Lh + \mathcal{P}(h + 1)(|\mathcal{A}| + k) \right) + \mathcal{P}Bkh + \mathcal{P}BhL \in \Omega(k)$$

I.2 LSTM Models

Let us consider an LSTM encoder model with weight precision \mathcal{P} bytes per unit, L layers, a hidden size of h , an action space size of $|\mathcal{A}|$, an inference batch size of $B_{\text{Inference}} = 1$, and a learning batch size of $B_{\text{Learn}} = B$. We assume the input is already provided in the form of k embeddings of size h . Additionally, in the case of the Frame Stacking model, we assume that there is a linear output head with a value for each environment action in \mathcal{A} . Furthermore, in the case of the Adaptive Stacking model there is another linear output head with a value for each of the k memory eviction actions. The number of copies of the model G that needs to be stored in memory to compute updates during training depends on the learning optimizer. In the case of SGD, we only need to store a single gradient $G = 1$, whereas for the popular AdamW optimizer $G = 4$.

While it is well known that RNNs can have inference costs independent of the history length, we note that this only works in pure testing settings and is not relevant to the continual learning setting we explore in this work. The issue is that the historical examples must be re-encoded by the RNN if any update has happened to the network during this sequence.

I.2.1 Producing a Single Action

Compute of Frame Stacking. Each LSTM cell at a given time step performs operations for 4 gates: the input gate, the forget gate, the output gate, and the candidate cell update. Each gate for each item in the batch for each time-step requires a matrix multiplication with the input, a matrix multiplication with the last hidden state, an additive bias vector, and a cost per hidden unit of applying non-linearities. Thus for each of the L layers we need $8h^2 + 4h + 16h$ FLOPs. For the last linear layer at the last step we need $2h|\mathcal{A}|$ FLOPs. This then brings the total FLOPs for a single action generation to:

$$|c|_{a \sim \pi_\theta} = kL \left(8h^2 + 20h \right) + 2h|\mathcal{A}| \in \Omega(k)$$

Compute of Adaptive Stacking. For Adaptive Stacking, we must do two passes through the L layer LSTM and additionally produce a memory action with a final layer head requiring $2hk$ FLOPs. This then brings the total FLOPs for a single action generation to:

$$|c|_{a \sim \pi_\theta} = kL \left(8h^2 + 20h \right) + 2h(|\mathcal{A}| + k) \in \Omega(k)$$

Memory of Frame Stacking. As with the MLP network, $|w|_{a \sim \pi_\theta} \geq \mathcal{P}|\theta|$ where the total parameters can be decomposed as $|\theta| = |\theta|_{\text{LSTM}} + |\theta|_{\text{activation}} + |\theta|_{\text{stack}}$. The network consists of 4 gates in each layer, including two matrices with h^2 parameters and one bias vector with h parameters. So, there are $8h^2 + 4h$ parameters per layer, and $L(8h^2 + 4h)$ parameters in the L layers. The linear output layer then contains $(h + 1)|\mathcal{A}|$ parameters. The activation memory only needs to be stored at the current step during inference, requiring $\mathcal{P}hL$ bytes of memory. The stack itself requires $\mathcal{P}kh$ bytes of memory. So the total RAM requirement of the model can be lower bounded as:

$$|w|_{a \sim \pi_\theta} \geq \mathcal{P}L(8h^2 + 4h) + \mathcal{P}(h + 1)|\mathcal{A}| + \mathcal{P}hL + \mathcal{P}kh \in \Omega(k)$$

Memory of Adaptive Stacking. The Adaptive Stacking case only adds the additional output layer for memory actions, which has $(h + 1)k$ total parameters. So the total RAM requirement of the model can be lower bounded as:

$$|w|_{a \sim \pi_\theta} \geq \mathcal{P}L(8h^2 + 4h) + \mathcal{P}(h + 1)(|\mathcal{A}| + k) + \mathcal{P}hL + \mathcal{P}kh \in \Omega(k)$$

I.2.2 Producing a TD Update

Compute of Frame Stacking. To compute a TD update, we must perform two forward propagations for each item in the batch. The additional forward propagation is for computing the bootstrapping target using a target network that is the same size as the original network. The cost of a backward propagation should match that of a forward propagation, so it is clear that $|c|_{\text{TD}} = 3B|c|_{a \sim \pi_\theta}$. This then brings the total FLOPs for a TD batch update to:

$$|c|_{\text{TD}} = 3BkL(8h^2 + 20h) + 6Bh|\mathcal{A}| \in \Omega(k)$$

Compute of Adaptive Stacking. In the case of Adaptive Stacking, we must perform TD updates for both the environment actions and the memory actions. Thus, we again have the relationship that $|c|_{\text{TD}} = 3B|c|_{a \sim \pi_\theta}$. This then implies that the total FLOPs for a TD batch update to:

$$|c|_{\text{TD}} = 3BkL(8h^2 + 20h) + 6Bh(|\mathcal{A}| + k) \in \Omega(k)$$

Memory of Frame Stacking. During a TD update, we must also store the target network in memory, which has the same number of parameters as the original LSTM. We also must store the activations of the main network for all steps now to compute the gradients. Thus, we can lower bound the memory required as $|w|_{\text{TD}} \geq (2 + G)\mathcal{P}|\theta|_{\text{LSTM}} + \mathcal{P}B|\theta|_{\text{stack}} + \mathcal{P}BkhL$, meaning the total RAM requirement of the model can be lower bounded as:

$$|w|_{\text{TD}} \geq (2 + G)\left(\mathcal{P}L(8h^2 + 4h) + \mathcal{P}(h + 1)|\mathcal{A}|\right) + \mathcal{P}BkhL + \mathcal{P}Bkh \in \Omega(k)$$

Memory of Adaptive Stacking. We again have the fact that $|w|_{\text{TD}} \geq (2 + G)\mathcal{P}|\theta|_{\text{LSTM}} + \mathcal{P}B|\theta|_{\text{stack}} + \mathcal{P}BkhL$, but $|\theta|_{\text{LSTM}}$ is different for Adaptive Stacking because of the extra final layer for the memory policy. So the total RAM requirement of the model can be lower bounded as:

$$|w|_{\text{TD}} \geq (2 + G)\left(\mathcal{P}L(8h^2 + 4h) + \mathcal{P}(h + 1)(|\mathcal{A}| + k)\right) + \mathcal{P}BkhL + \mathcal{P}Bkh \in \Omega(k)$$

I.3 Transformer Models

Let us consider an Transformer model with weight precision \mathcal{P} bytes per unit, L layers, a hidden size of h , an action space size of $|\mathcal{A}|$, an inference batch size of $B_{\text{Inference}} = 1$, and a learning batch size of $B_{\text{Learn}} = B$. We assume the input is already provided in the form of k embeddings of size h . Additionally, in the case of the Frame Stacking model, we assume that there is an linear output head with a value for each environment action in \mathcal{A} . Furthermore, in the case of the Adaptive Stacking model there is another linear output head with a value for each of the k memory eviction actions. The number of copies of the model G that needs to be stored in memory to compute updates during training depends on the learning optimizer. For example, in the case of SGD, we only need to store a single gradient $G = 1$, whereas for the popular AdamW optimizer $G = 4$.

I.3.1 Producing a Single Action

Compute of Frame Stacking. We consider the analysis of the compute required for a typical Transformer from Narayanan et al. (2021). The compute cost $|c|$ of doing inference of the final hidden state over a batch size of B_{Inf} over tokenized inputs with a context length of k using a Transformer with L layers and a hidden size of h is $24LB_{\text{Inf}}kh^2 + 4LB_{\text{Inf}}k^2h$ the compute cost of the final logit layer producing values for each action in \mathcal{A} is $2B_{\text{Inf}}h|\mathcal{A}|$ only applied once per sequence. So we can lower bound the compute cost of producing a single action (i.e. $B_{\text{Inf}} = 1$) as:

$$|c|_{a \sim \pi_\theta} \geq 24Lh^2k + 4Lhk^2 + 2h|\mathcal{A}| \in \Omega(k^2)$$

It is a lower bound because we do not include any pre-Transformer layers needed to produce embeddings for the input. We also do not include actions and rewards as part of the interaction history, which would bring the context length to $k' = 3k - 2$. Additionally, we do not include any re-computation costs that make sense to incur when we are bound by memory rather than compute – here we assume we are compute bound.

Compute of Adaptive Stacking. For producing a single action with Adaptive Stacking, the new compute overhead comes from the addition of the memory action head that comprises an extra $2hk$ FLOPs. This then brings the total FLOPs for a single action generation to:

$$|c|_{a \sim \pi_\theta} \geq 24Lh^2k + 4Lhk^2 + 2h(|\mathcal{A}| + k) \in \Omega(k^2)$$

Memory of Frame Stacking. We now assume that we are memory bound and not compute bound and include the cost of storing the model of parameter size $|\theta|$ at precision \mathcal{P} where $|\theta| = |\theta|_{\text{Transformer}} + |\theta|_{\text{stack}} + |\theta|_{\text{activations}}$. In each Transformer layer, there are $4h^2$ parameters used to compute attention, $8h^2$ parameters used in the feedforward network, and $4h$ parameters used in the layer norm. If biases are used for all linear layers, there are an additional $9h$ parameters – we exclude these for now in the spirit of lower bounds as they do not change the asymptotic result in terms of k either way. The output layer then has $(h + 1)|\mathcal{A}|$ parameters, making $|\theta|_{\text{Transformer}} = L(12h^2 + 4h) + (h + 1)|\mathcal{A}|$. The memory used for the stack itself is $\mathcal{P}kh$. Additionally, the cost of activations $\mathcal{P}khL$ assuming full re-computations at each step. This results in a lower bound on the working memory cost of producing a single action:

$$|w|_{a \sim \pi_\theta} \geq \mathcal{P}L(12h^2 + 4h) + \mathcal{P}(h + 1)|\mathcal{A}| + \mathcal{P}B(L + 1)hk \in \Omega(k)$$

Memory of Adaptive Stacking. The main additional memory overhead of Adaptive Stacking is the output layer for the memory policy, which has $(h + 1)k$ parameters. This results in a lower bound on the working memory cost of producing a single action:

$$|w|_{a \sim \pi_\theta} \geq \mathcal{P}L(12h^2 + 4h) + \mathcal{P}(h + 1)(|\mathcal{A}| + k) + \mathcal{P}(L + 1)hk \in \Omega(k)$$

I.3.2 Producing a TD Update

Compute of Frame Stacking. To compute a TD update, we must perform two forward propagations for each item in the batch. The additional forward propagation is for computing the bootstrapping target using a target network that is the same size as the original network. The cost of a backward propagation should match that of a forward propagation, so it is clear that $|c|_{\text{TD}} = 3B|c|_{a \sim \pi_\theta}$. This then brings the total FLOPs for a TD batch update to:

$$|c|_{\text{TD}} \geq 3B \left(24Lh^2k + 4Lhk^2 + 2h|\mathcal{A}| \right) \in \Omega(k^2)$$

Compute of Adaptive Stacking. In the case of Adaptive Stacking, we must perform TD updates for both the environment actions and the memory actions. Thus, we again have the relationship that $|c|_{\text{TD}} = 3B|c|_{a \sim \pi_\theta}$. This then implies that the total FLOPs for a TD batch update to:

$$|c|_{\text{TD}} \geq 3B \left(24Lh^2k + 4Lhk^2 + 2h(|\mathcal{A}| + k) \right) \in \Omega(k^2)$$

Memory of Frame Stacking. To analyse the working memory requirements $|w|$ of producing a single action for a typical Transformer, we follow [Anthony et al. \(2023\)](#). We now assume that we are memory bound and not compute bound. During a TD update, we must also store the target network in memory, which has the same number of parameters as the original Transformer. Thus, we can lower bound the memory required as $|w|_{\text{TD}} \geq (2 + G)\mathcal{P}|\theta|_{\text{Transformer}} + \mathcal{P}B|\theta|_{\text{stack}} + \mathcal{P}B|\theta|_{\text{activations}}$, meaning the total RAM requirement of the model can be lower bounded as:

$$|w|_{\text{TD}} \geq (2 + G) \left(\mathcal{P}L(12h^2 + 4h) + \mathcal{P}(h + 1)|\mathcal{A}| \right) + \mathcal{P}B(L + 1)hk \in \Omega(k)$$

Memory of Adaptive Stacking. We again have the fact that $|w|_{\text{TD}} \geq (2 + G)\mathcal{P}|\theta|_{\text{Transformer}} + \mathcal{P}B|\theta|_{\text{stack}} + \mathcal{P}B|\theta|_{\text{activations}}$, but $|\theta|_{\text{Transformer}}$ is different for Adaptive Stacking because of the extra final layer for the memory policy. So the RAM requirement of the model can be lower bounded as:

$$|w|_{\text{TD}} \geq (2 + G) \left(\mathcal{P}L(12h^2 + 4h) + \mathcal{P}(h + 1)(|\mathcal{A}| + k) \right) + \mathcal{P}B(L + 1)hk \in \Omega(k)$$

Architecture	Memory Type	$ c _{a \sim \pi_\theta}$	$ c _{\text{TD}}$	$ w _{a \sim \pi_\theta}$	$ w _{\text{TD}}$
MLP or LSTM	Frame Stack	$\Omega(k^*)$	$\Omega(k^*)$	$\Omega(k^*)$	$\Omega(k^*)$
MLP or LSTM	Adaptive Stack	$\Omega(\kappa)$	$\Omega(\kappa)$	$\Omega(\kappa)$	$\Omega(\kappa)$
Transformer	Frame Stack	$\Omega(k^{*2})$	$\Omega(k^*)$	$\Omega(k^{*2})$	$\Omega(k^*)$
Transformer	Adaptive Stack	$\Omega(\kappa^2)$	$\Omega(\kappa)$	$\Omega(\kappa^2)$	$\Omega(\kappa)$

Table 4: Compute $|c|$ and memory $|w|$ requirements for computing actions $a \sim \pi_\theta$ and TD updates.